

Perspective

Colored radiative cooling: progress and prospects

Bin Xie ^{a, c}, Yida Liu ^{b, c}, Wang Xi ^b, Run Hu ^{b, *}^a School of Mechanical Science and Engineering, Huazhong University of Science and Technology, Wuhan 430074, China^b State Key Laboratory for Coal Combustion, School of Energy and Power Engineering, Huazhong University of Science and Technology, Wuhan 430074, China

ARTICLE INFO

Article history:

Received 1 February 2023

Received in revised form

4 April 2023

Accepted 4 April 2023

Available online 8 April 2023

Keywords:

Thermal radiation

Color appearance

Metamaterials

Photonic crystal

Nanoparticle

Textile

Thermal management

ABSTRACT

With the notable development of radiative cooling research and the continuous improvement of cooling effect, its practicability and application range have been widely concerned. However, conventional radiative coolers typically come in white, which can be undesirable because of aesthetic reasons and the potential of light pollution. Fortunately, a colored radiative cooler (CRC) has been developed and demonstrated as a solution that offers both vivid colors and impressive radiative cooling performance. In this perspective paper, the state-of-the-art colored radiative cooling technologies are reviewed. Starting with the brief introduction of the fundamental principles of radiative cooling and color appearance, the mutually restrictive relationship between the color appearance and radiative cooling effect will be discussed, followed by the balanced design strategies. Then, the emerging materials and structures of different coolers will be discussed from the point of view of photonic crystal-based, nanoparticle-based, and fiber-based CRCs. Finally, conclusions and prospects are outlined to further promote the development of CRCs.

© 2023 Elsevier Ltd. All rights reserved.

1. Introduction

Owing to the advantages of passivity, high efficiency, and zero energy consumption, radiative cooling has become a hot topic in the field of energy-saving and thermal management applications. For achieving nyctohemeral radiative cooling, there are mainly two aspects for its physical design: enhancing thermal radiation and restraining solar absorption of the objects. From the first point of view, thermal radiation, arisen from random energy level transitions in matter, will appear in any objects which is at finite temperature. Thus, it is the most common way for energy transport. Based on this, the outer space, at a temperature close to absolute zero, can be a perfect heat sink. Owing to the low transmittance of the sky atmosphere, most of the thermal radiation from the objects on earth to the outer space is blocked. However, in the atmospheric window (8–13 μm), the atmosphere is highly transparent for thermal radiation. Moreover, the atmospheric window is basically consistent with the peak wavelength range of the thermal radiation of terrestrial objects at normal temperature [1]. Therefore, by increasing the emissivity of the objects in this specific wavelength

range, a large amount of thermal radiation can be one-way exported to the deep space, thus greatly enhancing the radiative heat dissipation of the objects. There are typically two types of radiators that can realize this purpose. One is the near-black radiator, whose emissivity is high throughout the mid-infrared (MIR) thermal radiative spectrum. The other is the atmospheric window selective radiator, whose emissivity is only high in the atmospheric window. By comparison of these two radiators, the former gains a relatively high cooling power than the latter but it suffers from additional atmospheric returned thermal radiation, which restricts its minimum cooled temperature. Thus, to obtain efficient nyctohemeral radiative cooling effect, it is far from enough to only enhance the thermal radiation of objects and neglect the injection of solar energy. From the aspect of restraining solar absorption, unlike thermal radiation of low-temperature terrestrial, the solar energy is distributed in a short wavelength band (0.3–4 μm), which makes it possible for an object to strongly reflect solar radiation while simultaneously exhibit high emissivity within the atmospheric transparent window.

Based on the aforementioned principles, many radiative coolers with a novel structure have been demonstrated [2–18]. To achieve better cooling performance, these conventional radiative coolers usually maximize their solar reflectivity by using white materials or metal mirrors with high reflectivity at the solar spectrum, which in

* Corresponding author.

E-mail address: hurun@hust.edu.cn (R. Hu).^c These authors contributed equally to this work.

turn limits their scope of application with aesthetic considerations. Actually, high solar reflectivity or white color is not desired in most applications for aesthetic reasons or potential menace of light pollution [19]. To address this issue, the research on 'how to add different colors on radiative coolers' is urgently needed. Thanks to the recent advances of theory and technology in radiators, the colored radiative cooler (CRC), which simultaneously achieves specific color appearance and radiative cooling performance, has been proposed and demonstrated. The CRCs typically have a wavelength-selectively high absorptivity/reflectivity in the visible spectrum (0.38–0.76 μm) for exhibiting the desired color. Meanwhile, the solar spectrum excluding the visible wavelengths especially the near infrared (NIR) wavelengths (0.76–2.5 μm) which takes up to 51% of solar energy are reflected. In addition, similar to the conventional radiative coolers, the CRCs can emit strong thermal radiation within the atmospheric transparent window for effective radiative heat dissipation.

The CRCs are not only a significant scientific achievement in materials science but also a meaningful milestone in engineering applications. The CRCs can be better substitutes for commercial paints for buildings to save the energy consumed by space cooling and maintain aesthetics, simultaneously [20,21]. With proper CRC schemes, the cooling set-point of the indoor air conditioning refrigeration system can be potentially expanded, which is of great significance of energy saving. Because, for instance, the energy consumption of indoor cooling has accounted for about 15% of the total household electricity usage in the USA [22]. As such, CRCs are also suitable for automotive thermal management. Under the premise of meeting the requirements of different colors of cars, the effective radiative cooling performance can not only reduce the energy consumption of the air conditioner in the car while driving but also, in particularly, provide thermal protection for the parked car; thus, preventing material damage and chemical volatilization caused by high temperature inside the cabin [23]. In addition, CRCs can also be combined with wearable textiles to fabricate colored functional clothes for personal thermal management to improve the thermal comfort of some outdoor staffs, such as traffic police, fire fighters, construction workers, and so on, who may be exposed to the sun in a hot weather, thus having a risk of sunburn or heat stroke [21,24,25]. As such, CRCs can enable the functional clothes to add the aesthetic characteristic to better cater the market demand. As a derivative of radiative cooling, CRCs open the specific avenue of a broad range of applications, which will be a significant turning point from theoretical research to practical application of radiative cooling.

In this perspective paper, the recent advances in the topic of CRCs are reviewed with an emphasis on the emerging materials and strategies. Most of the structural strategies of CRCs inherit from the traditional radiative coolers in order to give the readers a general idea of different types of structural designs of CRCs, we depict three typical CRCs as shown in Fig. 1a–c. Similar to the traditional radiative coolers, CRCs originate from photonic crystal materials. By a rational arrangement design of the structure, almost any ideal spectrum can be realized in photonics crystals, which are usually regarded as the design paradigm of CRCs (Fig. 1a). Besides the photonic crystals, the functional nanoparticles dispersed in the matrix or self-stacked can also achieve a good effect of spectrum regulation, considering the manufacturing cost and the demand of a large-scale practical application of CRCs, the nanoparticle-based CRCs are becoming a new research hotspot (Fig. 1b). In addition, due to the increasing demand of radiative cooling in personal thermal management, the colored radiative cooling technology begins to be incorporated into wearable clothing; thus, the

fiber-based CRCs have emerged (Fig. 1c). The organization of this perspective is consistent with the three typical structures mentioned above. In the main text, firstly, the basic fundamental principles, which contain radiative cooling and color appearance, are introduced briefly, followed by a discussion of the key point of the colored radiative design, i.e. the trade-off between color appearance and radiative cooling performances. Next, the main part of the paper is focused on the state-of-the-art CRCs based on advanced materials and strategies like photonic crystal-based CRCs, nanoparticle-based CRCs, and fiber-based CRCs. Finally, we summarize and discuss the challenges and opportunities in this field and forecast the future directions in terms of materials, structures, and a performance trade-off.

2. Fundamental principles

Literally, there are two evaluation indices of colored radiative cooling, namely the cooling effect and color appearance, which will be introduced briefly in this section.

2.1. Radiative cooling

The energy exchange between the CRC and the external environment via thermal radiation is illustrated in Fig. 1d, where R_{vis} is the designed reflectivity in the visible spectrum for color exhibition, R_{NIR} is the reflectivity in NIR wavelengths, which is high for reducing solar heat, ϵ_{MIR} represents the emissivity in the MIR spectrum, which is high for radiative cooling. A designed reflectivity in the visible spectrum aims to yield a specific color, while the NIR wavelengths are highly reflected for reducing solar absorption, and high emissivity in the MIR spectrum is used for maximizing radiative cooling performance. More specifically and quantitatively, the net cooling power density, P_{cool} , can be expressed as [11]:

$$P_{\text{cool}}(T) = P_{\text{rad}}(T) - P_{\text{atm}}(T_{\text{amb}}) - P_{\text{solar}}(\theta) - P_{\text{cond+conv}} \quad (1)$$

Where, T and T_{amb} represent the temperature of the CRC and ambient, respectively, and θ is the angle of radiation. $P_{\text{rad}}(T)$ represents the outward radiation power density of the CRC, which can be calculated as

$$P_{\text{rad}}(T) = \int d\Omega \int_0^{\infty} I_{\text{BB}}(T, \lambda) \epsilon(\lambda, \theta) \cos \theta d\lambda \quad (2)$$

Where, $\int d\Omega = \int_0^{\pi/2} d\theta \sin \theta \int_0^{2\pi} d\varphi$ is the angular integral over a hemisphere, $I_{\text{BB}}(T, \lambda) = \frac{2hc^2}{\lambda^3 e^{hc/\lambda k_B T} - 1}$ is the spectral radiance of a black body at temperature T , where λ is the wavelength, h is the Planck's constant, c is the light speed, and k_B is the Boltzmann constant, and $\epsilon(\lambda, \theta)$ is the emissivity of the CRC. Based on Kirchoff's law, the emissivity of the CRC is equal to its absorptivity under circumstances of thermal equilibrium. $P_{\text{atm}}(T_{\text{amb}})$ is the power density of the atmospheric radiation absorbed by the CRC, which is given by

$$P_{\text{atm}}(T_{\text{amb}}) = \int d\Omega \int_0^{\infty} I_{\text{BB}}(T_{\text{amb}}, \lambda) \epsilon(\lambda, \theta) \epsilon_{\text{atm}}(\lambda, \theta) \cos(\theta) d\lambda \quad (3)$$

Where, $\epsilon_{\text{atm}}(\lambda, \theta) = 1 - \tau(\lambda)^{1/\cos \theta}$ is the emissivity of the atmosphere, and here, $\tau(\lambda)$ is the atmospheric transmittance in the zenith direction [26]. $P_{\text{solar}}(\theta)$ stands for the solar energy absorption of the CRC, which can be calculated by [27,28]

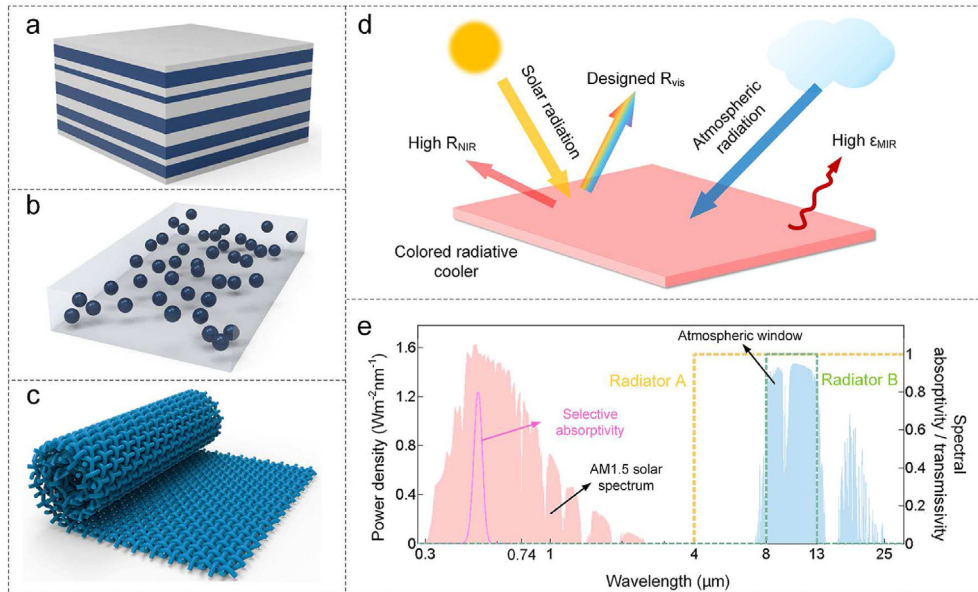


Fig. 1. The schematic diagram of a) photonic crystal, b) nanoparticle, and c) fiber-based CRCs. d) The schematic showing the interaction between external radiation and self-radiative properties of CRCs. e) Radiative characteristic curves of different ideal radiators. CRC, colored radiative cooler.

$$P_{\text{solar}}(\theta) = G \frac{\int_0^{\infty} \varepsilon(\lambda, \theta) I_{\text{AM1.5}}(\lambda) d\lambda}{\int_0^{\infty} I_{\text{AM1.5}}(\lambda) d\lambda} \quad (4)$$

where, $I_{\text{AM1.5}}(\lambda)$ denotes the standard AM 1.5 spectrum of solar radiation, and G is the total solar irradiance, which is about 1 kW/m^2 [29]. However, the actual solar irradiance G_a always changes under different circumstances or at different times. Thus, the calculation of solar irradiance in an actual situation is usually preceded by the addition of a correction term as $\frac{G_a}{G} P_{\text{solar}}$ [29]. In addition to radiative factors, non-radiative factors, including thermal convection and thermal conduction, also affect the radiative cooling effect, and the corresponding power density is

$$P_{\text{cond+conv}} = h_c(T_{\text{amb}} - T) \quad (5)$$

Where, $h_c = h_{\text{cond}} + h_{\text{conv}}$ combines the equivalent non-radiative heat-transfer coefficients of thermal conduction and convection. Equations (1)–(5) are the typical procedure of the evaluation of the radiative cooling performance, and more attention should be paid to control the solar energy absorption. In the daytime, the actual solar irradiance can reach about $800\text{--}1,100 \text{ kW/m}^2$, which is almost two to three times the total thermal radiation of terrestrial objects at room temperature. Therefore, protection against solar radiative energy is the key to achieve daytime radiative cooling, especially for CRCs, which have to sacrifice part of the cooling capacity in the solar spectrum for color appearance.

2.2. Color appearance

The color appearance of different objects mainly depends on two ways, one is active color and the other is passive color. The active color originates from the luminescence process of self-luminous materials, such as a fluorescent lamp [30], upconversion materials [31,32], a light emitting diode [33–35], etc. These materials can be transformed into an excited state after being

stimulated, and the energy of the excited state will be released as electromagnetic waves in a visible band, eventually. Different materials require different stimuli for active color appearance, such as electroluminescence [36–38], photoluminescence [39,40], thermoluminescence [41,42], etc. These strategies for active color appearance can form different colors without the absorption of the external solar energy, which is an excellent method for CRCs. However, these self-luminous materials still suffer from their operating conditions of additional stimuli, which greatly limit their application in CRCs, and few studies have been reported in this field so far. As for passive color, it is the most common way for color appearance in nature, which depends on two forms. The first one is pigmentary color, which refers to the color produced by the absorption or reflection of light by a single substance such as pigments. The other is the structural color, which results from the interference of light scattered by judiciously distributed nanoscale or microscale structures [43]. Though the pigmentary color produced by ordinary pigments is a good choice for color appearance, the radiative properties of pigments are poorly selective and difficult to control, which will lead to extra solar energy absorption and thus impairs or even disrupts the radiative cooling function in CRCs. By contrast, the structural color supported by photonic crystal- or particle-based structures is more applicable to CRCs because the judiciously optical structures can achieve a high solar spectral selectivity, which makes it possible for them to exhibit specific colors while reflecting the extra solar energy, thus achieving a better function of radiative cooling.

After the definition of the structures for color appearance, the quality of the color should be evaluated. The ability of human to recognize different colors mainly counts on the synergistic interaction of the spectral reflectivity spectrum from the objects, the spectral intensity of the light source, and the sensitivity of the three cone cells in human eyes. In CIE systems, the sensitivities of the three cone cells are denoted by the optical primary color matching functions, $\bar{x}(\lambda)$, $\bar{y}(\lambda)$, and $\bar{z}(\lambda)$ [44]. Further, the stimulus values of the primary colors, i.e. the tristimulus values, X , Y and Z , can be calculated as

$$X = 100 \frac{\int s(\lambda)R(\lambda)\bar{x}(\lambda)d\lambda}{\int s(\lambda)\bar{y}(\lambda)d\lambda} \quad (6)$$

$$Y = 100 \frac{\int s(\lambda)R(\lambda)\bar{y}(\lambda)d\lambda}{\int s(\lambda)\bar{y}(\lambda)d\lambda} \quad (7)$$

$$Z = 100 \frac{\int s(\lambda)R(\lambda)\bar{z}(\lambda)d\lambda}{\int s(\lambda)\bar{y}(\lambda)d\lambda} \quad (8)$$

Where, $s(\lambda)$ is the spectral power distribution of the illuminant and $R(\lambda)$ is the spectral reflectivity of the objects. For self-luminous materials, $R(\lambda)$ is defined as 1. The lightness of the color can be simply determined by the parameter Y , while the chromaticity is determined by the normalized parameters, x , y , and z

$$x = \frac{X}{X + Y + Z} \quad (9)$$

$$y = \frac{Y}{X + Y + Z} \quad (10)$$

$$z = \frac{Z}{X + Y + Z} \quad (11)$$

In which, x and y are used as horizontal and vertical coordinates, respectively, to locate corresponding chromaticity in the CIE 1931 color space. However, in the colored radiative cooling, the difference between the actual structure color and the target color is also an important parameter to evaluate the effect of colored radiative cooling. Thus, another CIE LAB color space which is able to identify the color difference is introduced, where L represents the lightness, a represents redness and greenness, and b represents yellowness and blueness. The tristimulus values, X , Y , and Z , can be transformed into L , a , and b by the following equations [45]

$$L = 116f(Y/Y_0) - 16 \quad (12)$$

$$a = 500[f(X/X_0) - f(Y/Y_0)] \quad (13)$$

$$b = 200[f(Y/Y_0) - f(Z/Z_0)] \quad (14)$$

Where, X_0 , Y_0 , and Z_0 are the tristimulus values corresponding to white, and

$$f(s) = \begin{cases} t^{\frac{1}{3}}, & t > \left(\frac{24}{116}\right)^3 \\ \left(\frac{841}{108}\right)t + \frac{16}{116}, & t \leq \left(\frac{24}{116}\right)^3 \end{cases} \quad (15)$$

then, the color difference between two colors can be obtained as

$$\Delta E = \sqrt{(\Delta L)^2 + (\Delta a)^2 + (\Delta b)^2} \quad (16)$$

Here, the radiative properties of four ideal radiative coolers, including conventional radiative coolers and colored radiative coolers, are presented in Fig. 1e for intuitively demonstrating the differences between different coolers. Radiator A is a broaden band

cooler with high emissivity in the entire MIR spectrum, while radiator B is a narrow band selective radiator with emissivity only high in the atmospheric transparent window. Owing to the strong reflectivity within the solar spectrum, the conventional radiative cooler A and B possess high cooling power with a white color. The other two ideal CRCs with a passive color are created by introducing a selective absorption peak in the visible spectrum of the radiator A and B for color appearance, which, in turns limits the cooling power. The restrictive correlation and balanced trade-offs between the color appearance and the cooling effect are discussed in the next section in details.

3. Color appearance vs. radiative cooling

A common CRC can be divided into a radiative cooling module and a color appearance module. The former mainly determines the cooling performance, while the latter manipulates the color. The existing CRCs can be classified into photonic crystal-based, nano-particle-based, and fiber-based coolers. Some excellent works based on a multilayer photonic crystal have found that the color display and radiative cooling performance of a CRC are mutually restricted. It is reasonable because the requirement of reflectivity in the visible waveband is contrary for the color display and radiative cooling. Radiative cooling requires as large reflectivity in the visible band as possible to limit input solar radiation. However, a vivid color requires a specific reflectivity spectrum to display color. For example, a magenta structural color needs a reflectivity dip, also an emissivity peak at 500 nm, which will lead to more solar radiation absorption, weakening or even damaging the radiative cooling performance. Our work further explores their relation by taking the Ag-SiO₂-Ag multilayer color display module as an example [46]. As shown in Fig. 2a, we compared a conventional white-color radiative cooler consists of the SiO₂/TiO₂ photonic crystal with a light-magenta-color one with the color display module added. The former can maintain a subambient temperature of 12.76 °C, while 9.44 °C for the latter. Both the emissivity spectrum as well as the power of energy inflow and outflow recorded in the table show that the increase of input solar radiation in the visible band is dominant in the competing role between the color display and radiative cooling. Fig. 2c shows the corresponding color types under different steady-state temperatures, which not only provide reference for practical application but also demonstrate what roles the key parameters play in controlling color and cooling, with the conclusion that the upper Ag layer thickness mainly influences the radiative cooling effect, while the SiO₂ layer thickness controls the color display. Additional discovery comes with Fig. 2b that the reflectivity of the visible band can be divided into peak-types and valley-type according to the thickness of the Ag layer (d_{Ag}) and SiO₂ layer (d_{SiO_2}), with great differences in their radiative cooling performance and color display. However, no matter which mode is, the brightness of color and radiative cooling performance have a significant positive correlation, as depicted in Fig. 2d, which points out an intuitive relation between them. Faced with the dilemma between color appearance and radiative cooling, there is no choice but compromise between the richness of color and cooling power. Either way, the key is to design a delicate structure and manipulate the solar radiation absorption properly.

4. Photonic crystal-based CRC

With the development of advanced design and fabrication technology, photonic crystals have been widely used in radiative coolers [47]. As for CRCs, the photonic structures are usually divided into two parts, which are used to adjust the radiative cooling properties and color appearance, respectively. By a rational

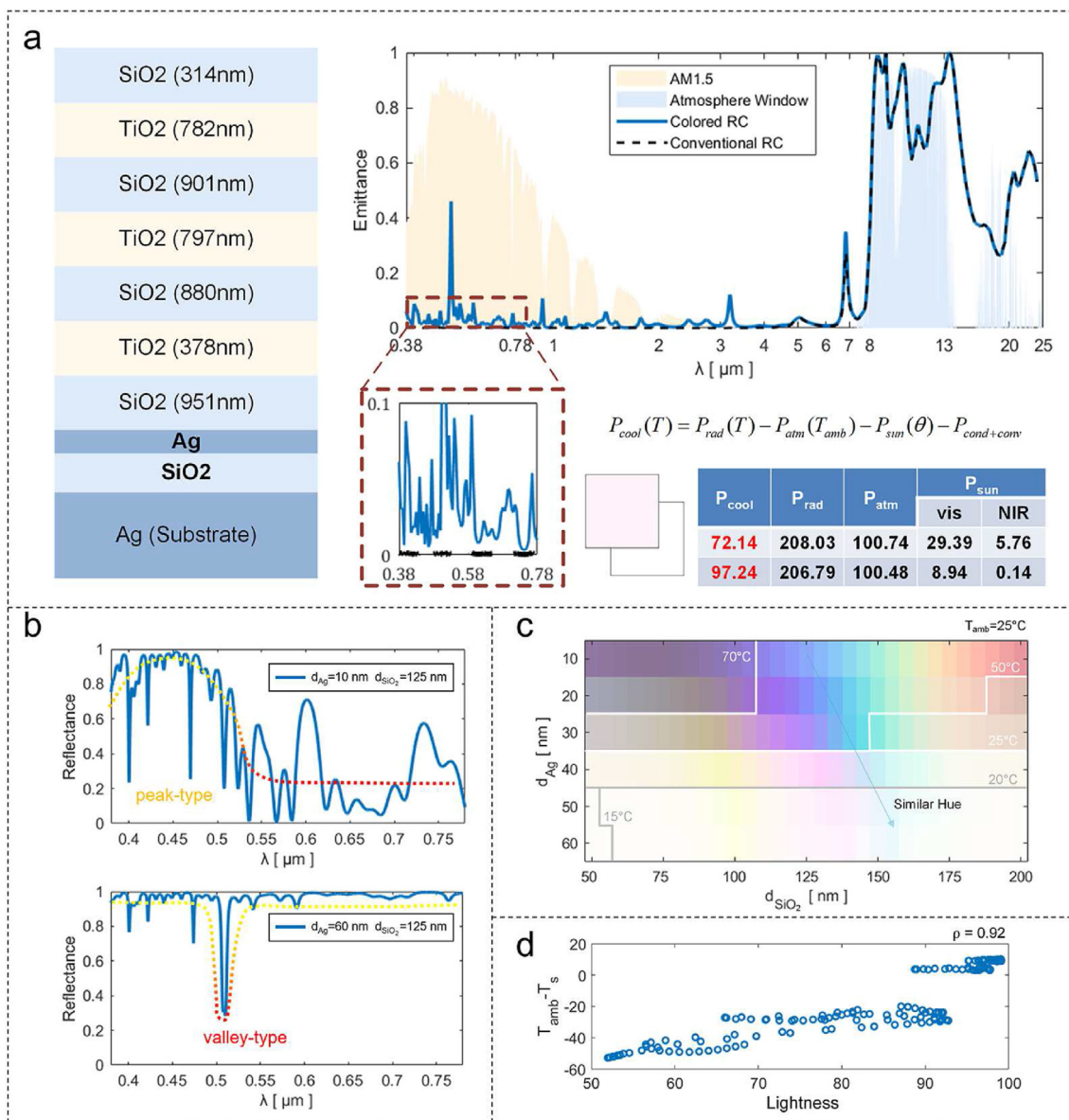


Fig. 2. a) A typical CRC structure and its performance. b) Peak-type and valley-type reflectivity in the visible band. c) The color and steady-state temperature with different structural parameters. d) Correlations between the lightness and temperature difference between ambient and the cooler [46]. CRC, colored radiative cooler.

distribution of the periodic structure, including the patterned structure and multilayered structure in photonic crystal schemes, the special radiative properties in CRCs can be achieved. Owing to the structural diversity and the easily combinative characteristic, photonic crystals have great potential of improving the colored radiative cooling effect.

4.1. Patterned CRC

Patterned photonic crystals, a branch of the optical metamaterials, are a good platform for tailoring the complex spectral properties in radiative cooling as well as structural colors due to their high structural degree of freedom [48]. It has been demonstrated that metal-dielectric metamaterials can exhibit some intriguing optical properties [49,50]. Inspired by this, researchers have proposed various radiative coolers based on the metal-dielectric metamaterials [6,12,51,52]. Among them, Rephaeli et al.

firstly presented a metal-dielectric photonic crystal with a high reflectivity in the solar spectrum and a high emissivity within the atmospheric window by using a double-layer quartz-silicon carbide (SiC) patterned photonic crystal combined with a chirped multilayered reflector [12]. As shown in Fig. 3a, the quartz and SiC were designed and placed as the top two layers of the cooler to realize strongly selective thermal emission in the atmospheric window, so as to maximize the radiative cooling power. Simultaneously, a one-dimensional (1D) photonic crystals-based reflector consisting of alternating layers of TiO₂ and MgF₂ was introduced below the quartz-SiC structure to minimize the absorbed solar radiation. Consequently, the calculated net cooling power of this structure exceeds 100 W/m². Similar to the former concept, Hossain et al. fabricated a patterned photonic crystal consisting of a symmetrically shaped conical metamaterials pillars array (Fig. 3b), where each pillar is composed of alternating layers of Ge and Al, reaching a nearly ideal emission within the atmospheric window [6]. As a

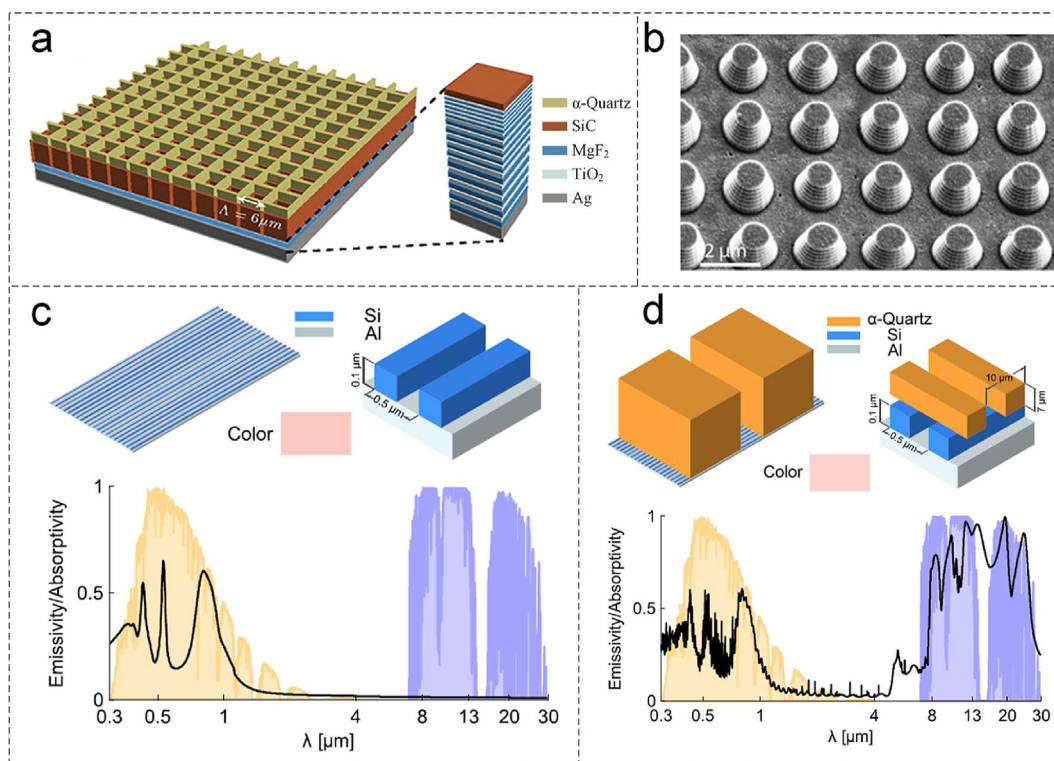


Fig. 3. a) A daytime radiative cooler consisting of quartz-SiC thermally emitting photonic crystal layers [12]. b) The SEM image of the CMM pillars [6]. c), d) Schematic and emissivity/absorptivity spectra of the colored CRC [53]. CMM, conical metamaterial; CRC, colored radiative cooler; SEM, scanning electron microscope.

result, this structure demonstrated the ability to cool down 12.2 °C and 9 °C below the ambient temperature at nighttime and daytime, respectively, even in the presence of convective and conductive heat exchange. These are some typical patterned photonic crystals only with a view to radiative cooling.

Taking the extra color appearance into consideration, Zhu et al. introduced a general approach for producing a daytime CRC based on a double-layer patterned photonics crystal [53]. As shown in Fig. 3c and d, the patterned cooler can be divided into two functional units. At the bottom is the colored unit (Fig. 3c), which is composed of a periodic array of Si nanowires on an Al substrate. The structure color can be changed by tuning the side length and periodicity of the Si nanowires as the Si nanostructure can exhibit different colors by their geometric properties [54]. The other radiative cooling unit, periodic array quartz bars stacked on the top of the Si nanowires, is transparent in the solar spectrum, while preserving high emissivity within the atmospheric window (Fig. 3d). Thus, the whole structure can effectively achieve radiative cooling while barely affecting its color quality. For the first time, radiative cooling has been studied in conjunction with the color performance. This study has put forward a new research idea for radiative cooling, which has made a great contribution to its development in applications.

4.2. Multilayered CRC

Although patterned structures can facilitate the design of the stringent radiative properties in radiative cooling, the complicated structures raise huge difficulties for manufacturing and subsequent applications. A multilayered structure, a 1D photonic crystal consisting of alternating layers of different materials, is a good approach to simplify the structural design in radiative cooling, which improves the feasibility of manufacturing and application of

the coolers [55]. The subambient radiative cooling was first achieved by Raman et al. based on a multilayered structure. The cooler consists of seven alternating layers of hafnium dioxide (HfO_2) and SiO_2 , on top of a 200 nm Ag substrate deposited on a 200 mm Si wafer, which reflects 97% of the solar energy while strongly emitting within the atmospheric window [11]. It has been demonstrated that the cooler can exhibit a 4.9 °C subambient temperature when exposed to direct sunlight. In order to further optimize a multilayered radiative cooler and improve its cooling effect, Kou et al. demonstrated a polymer-coated fused silica mirror, which consists of fused silica water sandwiched by a polydimethylsiloxane (PDMS) top film and an Ag back reflector [9]. This simple scheme is able to reflect most of the incident sunlight, while regarded as a near-black radiator in the MIR spectrum, thus, achieving 8.2 °C and 8.4 °C subambient temperatures in daytime and nighttime, respectively.

Based on previous researches, the color function of radiative cooling has been realized by using a similar multilayered photonic crystal. Song et al. fabricated a multilayered CRC with subtractive primary colors (i.e. yellow, cyan, and magenta) [56]. The schematic of the multilayered CRC is shown in Fig. 4a, it consists of SiO_2 /silicon nitride (Si_3N_4) selective emitters (SEs) possessing high emissivity within the atmospheric transparency window on the top and an Ag/ SiO_2 /Ag metal-insulator-metal (MIM) scheme for the color appearance on the bottom. In the MIM scheme, different colors can be obtained by varying the thickness of the insulator layer to tune the interference effect in 1D-stacked layers. In outdoor experiments, the multilayered CRC has shown excellent radiative cooling at an average temperature, 3.9 °C, lower than the ambient temperature. In addition, the multilayered CRC exhibits a certain degree of softness due to its ultrathin structural features, which makes it an effective cooling material for wearable electronics. After combined with an Al foil and encapsulated with PDMS, the flexible radiative cooling material shows a strong flexibility. As

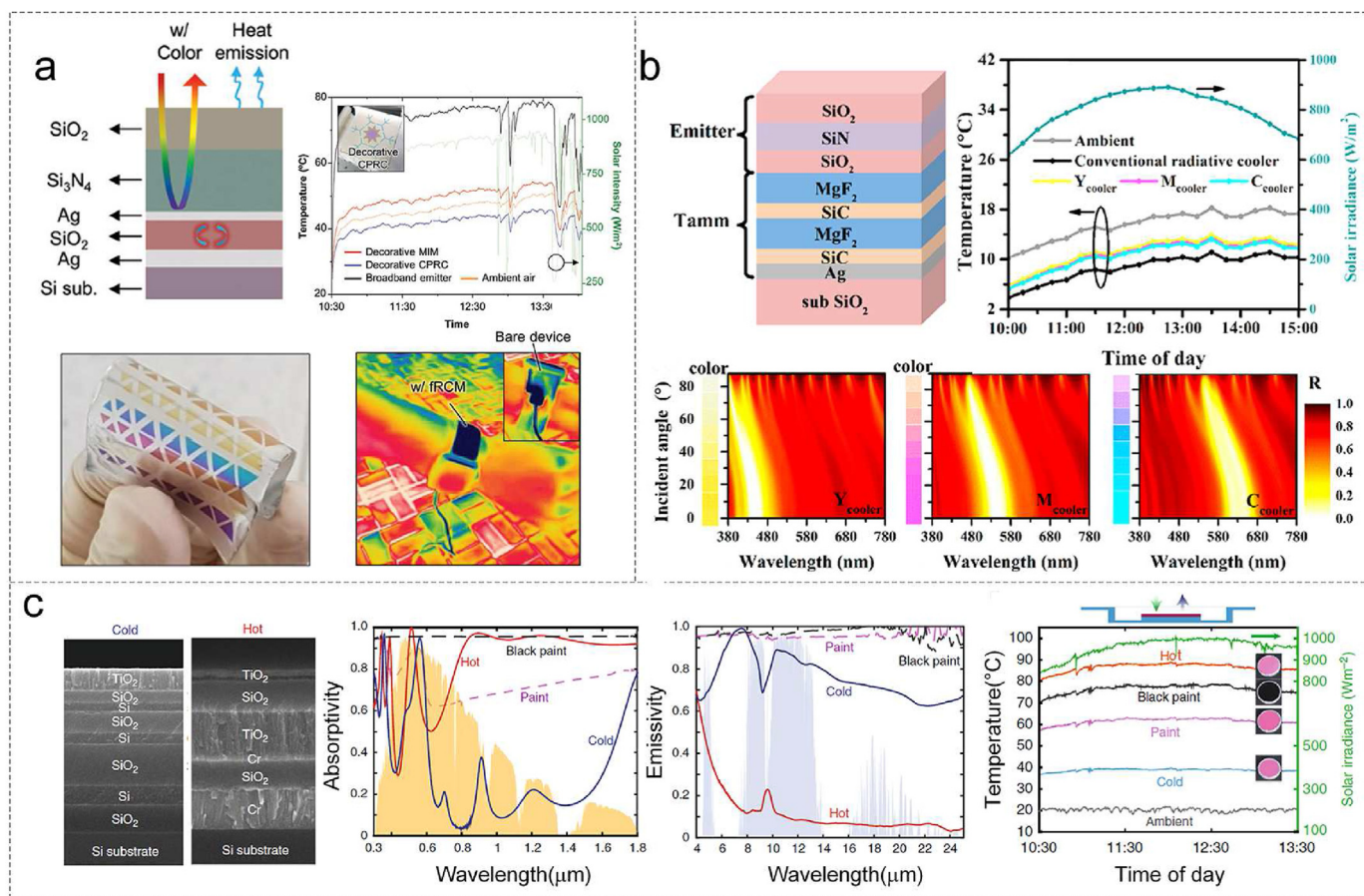


Fig. 4. a) The structure and temperature variation of the multilayered CRC during the daytime [56]. b) The structure of the CRC, and simulated temperatures of the conventional cooler and CRCs [29]. c) Cross-section SEM images and absorptivity/emissivity spectra of the cold photonic structure and the hot photonic structure [63]. CRC, colored radiative cooler; SEM, scanning electron microscope.

demonstrated in the smart watch cooling tests, the temperature of the watchband covered with the flexible radiative cooling material is 5–11 °C, lower than the bare one when exposed to the sunlight, which verifies that the CRC is also effective in the thermal management of wearable electronics. Though the MIM scheme can produce different colors via an interference absorption peak, it still suffers from the dearth of color options, i.e. only three subtractive primary colors can be obtained owing to the single absorption peak supported by MIM. To extend the gamut of CRC, it is necessary for the color display module to produce more absorption peaks. Fortunately, some recent works have proved that multilayer structures consist of several MIM structures can produce multiple interference peaks [57,58]. Inspired by this, Blandre et al. proposed a CRC with extended gamut [59]. Similar to the multilayered CRC mentioned above, the CRC is composed of a SE on the top and a color display module on the bottom, in which the SE is composed of a SiO₂ layer with a cubic SiO₂ grating array on the top, which greatly enhances the emissivity of SiO₂ in the atmospheric window. In the color display module, a double MIM scheme is applied, which consists of two HfO₂ layers sandwiched between three Ag layers. Owing to the multiple interference effect, two absorption peaks have been obtained in the visible spectrum, which can be tuned by varying the thickness of the Ag or HfO₂ layer. In this way, CRCs with various colors can be achieved, which greatly expands their application domain.

Most CRCs sacrifice a large amount of the cooling effect to display a specific color, and the color is still light or uneven with

strong angular dependence. A Tamm structure can be a candidate to fix this problem. Optical Tamm states are confined optical modes that occur at the interface between two highly reflective structures, which have risen as an effective strategy for light confinement. Under optical Tamm states, a specific reflectance dip can be easily controlled to obtain a pure color. Moreover, a Tamm structure has the advantage of low dependence on an incident angle, can thus be utilized to fabricate angle-insensitive absorption structures [60]. Li et al. proposed a CRC under optical Tamm resonance with high-purity subtractive primary colors [29]. As shown in Fig. 4b, the cooler is composed of a conventional SiO₂–SiN–SiO₂ SE and a Tamm structure consists magnesium fluoride (MgF₂)/SiC on the top of the Ag film [61,62]. By optimizing the layered material thickness distribution in the Tamm structure, the selective reflectivity in the visible spectrum can be obtained for high-purity color appearance, while high emissivity is preserved within the atmospheric window. Moreover, the angular performance evaluation indicates that the cooler can keep the initial hue well sustained even until the incident angle reaching 70°. In thermal calculation, the cooling power of CRCs can reach 44–52 W/m², resulting in a 5–6 °C subambient temperature. The high-purity color and the effective radiative cooling are achieved simultaneously in the Tamm structure, which brings a new idea in CRC design.

The color of an object is only affected by its radiative properties in the visible spectrum, in this way, the radiative thermal load of objects can be tuned by adjusting the radiative properties of the NIR and MIR spectrum while preserving the same color. As shown in

Fig. 4c, Fan et al. discussed the tunable range of the theoretical radiative thermal load of objects with the same color for radiative cooling or heating issues and demonstrated the theory by experiment [63]. The authors calculated the theoretical limit values of the radiative thermal load in different colors and found a wide tunable range over the entire color space with a minimum of 680 W/m^2 and a maximum of 866 W/m^2 . Based on these findings, they fabricated two multilayered samples with drastically different radiative thermal loads while maintaining the same pink color by different structure designs. The pink radiative cooler is tailored to reflect solar energy as much as possible while strongly emitting in the entire MIR spectrum, whereas the radiative properties of the pink radiative heater are exactly opposite. Outdoor experiments show that the cooler is 22.6°C colder than the normal pink paint sample, whereas the heater is 25°C hotter than the paint sample, which elucidates great potential of CRCs in photonic thermal management and thermoelectric applications.

Displaying deep colors (such as black) while maintaining sub-ambient temperature is still challenging for the state-of-the-art CRC. Recently, Jeon et al. proposed a radiatively intertwined non-equilibrium system that may solve the conflict between color appearance and radiative cooling [64]. This system consists of an outer-most spectrally selective filter, a selective heat transfer layer in the middle, and a thermal emitter at the back of the objects to be cooled. It ensures that the internal emitter can release radiative heat to outer space but to be insulated from the radiative and non-radiative heat sources outside. As a proof of concept, an even-black cooler, which absorbs 646 W/m^2 of solar power, could be cooled down to a maximum 6.9 K of subambient temperature during the daytime. This system has expanded the diversity of color aesthetics as well as the commercial feasibility of conventional CRCs.

5. Nanoparticle-based CRC

As the dimension of a material shrinks from a macroscopic scale to a microscopic scale, its optical properties may be slightly changed [28]. For instance, the phonon-polariton resonances in bulk SiO_2 can lead to a reflection peak. However, this effect can be converted into a strong absorption in SiO_2 nanoparticles, which makes it easy to meet the radiative properties demands in CRCs by regulating the nanoparticle geometry properties. What's more, compared with complex photonic crystal structures, nanoparticle-based structures are also more processable. Due to the flexible and adjustable radiative properties and the easy-to-craft merit, nanoparticle-based materials have become one of the ideal materials for CRCs.

5.1. Nanoparticles/matrix CRC

Introducing randomness into the photonic system is an effective way to amplify spontaneous thermal emission [65,66], which makes a nanoparticle/polymer a potential candidate material for radiative cooling. The nanoparticles can be regarded as randomly distributed optical resonators when encapsulated with polymers; meanwhile, polymeric matrix is attractive for scalability and economy [67,68]. Yang et al. fabricated a glass-polymer hybrid film for daytime radiative cooling [14]. The film is composed of a SiO_2 /polymethylpentene emitter, which is highly emissive within the entire atmospheric window owing to the phonon-enhanced Fröhlich resonances of the SiO_2 nanoparticles, and an Ag back reflector. Although the Ag can be an excellent material in radiative cooling for its high solar reflectivity, it is too expensive for further applications. The light-scattering air nanovoids, which we also classify as nanoparticles, can eliminate this problem while keeping effective radiative cooling performance. Yang et al. reported a

simple and scalable process for fabricating hierarchically porous poly(vinylidene fluoride-co-hexafluoropropene) [P(VdF-HFP)]_{HP} coatings [10]. The induced micropores and nanopores in the polymeric matrix efficiently backscatter sunlight and enhance emission in the MIR spectrum. What's more, the porous coatings facilitate incorporating dyes, which show immense potential in colored radiative cooling.

To further implement the colored function of the radiative cooler, after two years, Yang et al. demonstrated colored and paintable bilayer coatings [69]. As shown in Fig. 5a, the top layer is the normal commercial paints, which selectively absorb sunlight for desired color appearance, while the underlayer is a porous P(VdF-HFP) or titanium dioxide (TiO_2)/polymer composite membrane, which is aimed at maximizing the backscattering of the sunlight transmitted by the top layer. Thus, the other visible and NIR light can be strongly reflected, while the polymer materials and colored paints are ideal emitters for their intrinsic high emissivity in the MIR spectrum. Compared with conventional monolayer cooling paints, bilayer CRCs attain higher NIR reflectivity and can stay cooler by as much as $3\text{--}15.6^\circ\text{C}$ when exposed to strong sunlight. By introducing conventional paints in the structural design, bilayer CRCs can achieve a wide range of color selection. However, the normal commercial paints are not ideal materials for color appearance since the colorant in paints is absorptive in the NIR spectrum, which is not only profitless to color but also detrimental to radiative cooling performance.

In order to mitigate the color absorptive loss in radiative cooling, the highly selective narrowband absorption in the visible spectrum is required. In Fig. 5b, Drevillon et al. proposed a coating composed of nanoparticles embedded in a SiO_2 matrix applied on an Ag reflector [70]. Owing to the localized surface plasmon resonances, the SiO_2 matrix embedded with Ag-based nanoparticles can exhibit ideal narrow absorption peaks in the visible spectral region, while SiO_2 is highly emissive within the atmospheric window. It is found that the coatings embedded with plain Ag nanoparticles and SiO_2 core-Ag shell nanoparticles are able to exhibit yellow and subtractive primary colors with a proper particle size, respectively. Similar to the subtractive color mixing process, multiple absorption peaks in the visible spectrum can be obtained when nanoparticles with different geometries are mixed. Thus, various colors can be achieved in CRCs, like green, purple, and red. For a specific color, the saturation is in competition with the radiative cooling effect as purer colors represent higher corresponding absorption peaks in the visible region. Based on the nanoparticles/matrix structure, the CRC provides a very intuitive way to control the color over a wide range, while greatly reducing the negative effect of color absorption on radiative cooling.

The highly selective absorption spectrum can restrain the absorption of solar energy in the process of color appearance for CRCs; however, due to the mechanism of passive color, the object will absorb a certain amount of solar energy in any case, which in turn deteriorates its radiative cooling effect. Based on this issue, Lee et al. creatively proposed multifunctional layers with a simultaneous active light-emitting color and radiative cooling function [71]. The CRC is composed of a substrate upon which a thin Ag film is deposited and a SiO_2 coated- CsPbX_3 ($X = \text{Br}, \text{I}$) nanocrystals/PDMS (CPB@PDMS) composite layer. The CsPbX_3 perovskite nanocrystals can emit bright and colorful light under ultraviolet (UV) or blue illumination with a high photoluminescence quantum yield [72,73], which makes them a highly suitable material for CRCs with active color. In the CPB@PDMS layer, the content of the CsPbX_3 nanocrystals has been carefully controlled, allowing it to be highly transparent at visible wavelengths and exhibit sufficient color intensity under UV light. In the outdoor experiments, the CRCs achieved a $6\text{--}7.4^\circ\text{C}$ subambient temperature drop, as shown in Fig. 6a.

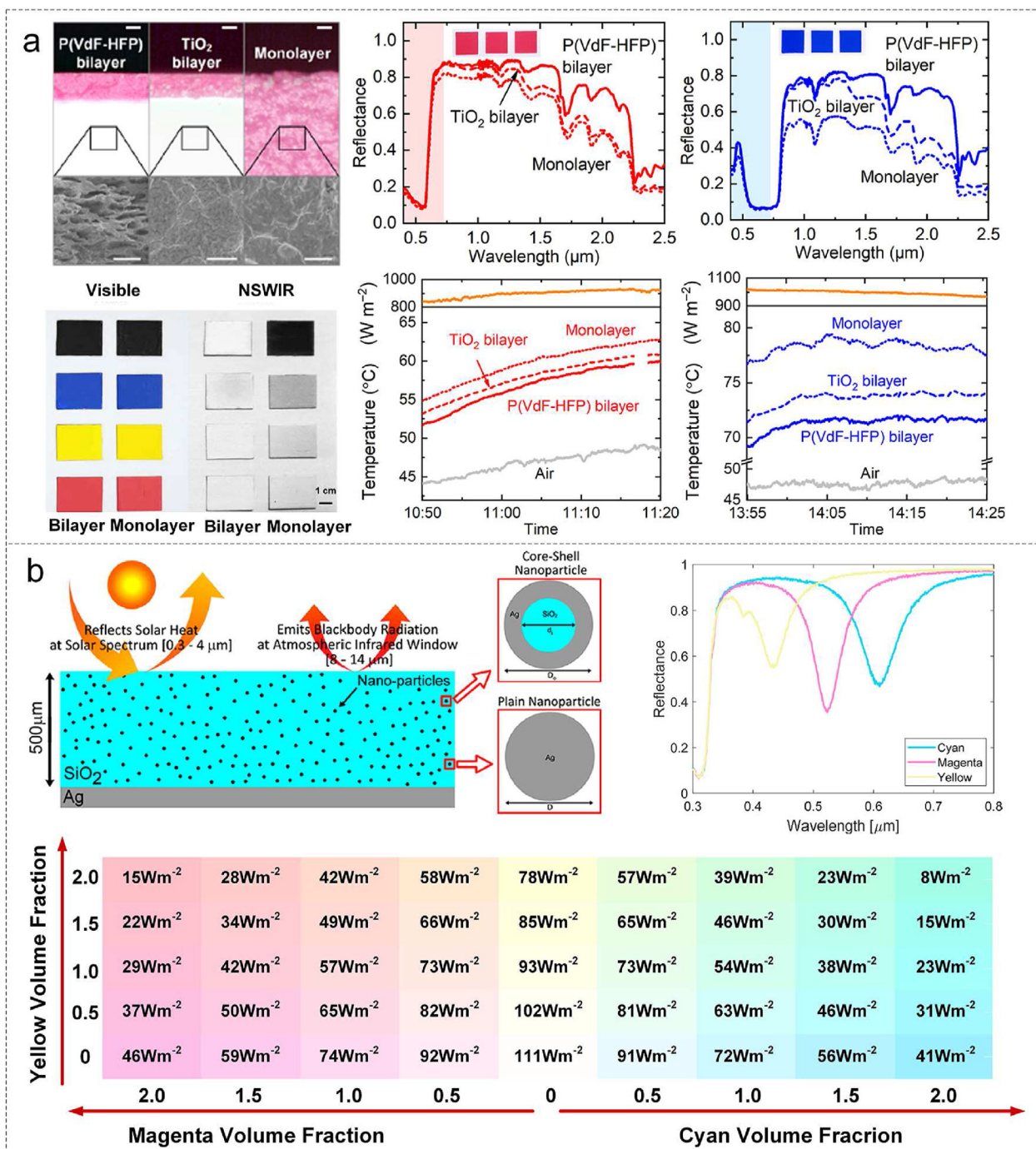


Fig. 5. a) The porous P(VdF-HFP) CRC, TiO₂/polymer CRC, and monolayer coating with different colors [69]. b) Structure and opto-thermal properties of CRCs with different colors [70]. CRC, colored radiative cooler.

The multifunctional CRC adopts active luminescence as the method for color appearance without degrading its cooling performance, which opens a new avenue for the CRC design [74]. However, it is still in a development stage, and many problems remain unsolved. For example, self-luminous materials require additional stimuli, which means extra energy consumption, and the luminous effect of the materials is only significant at night but not at day.

Considering the above-mentioned limitations, Lee et al. further optimized the structure and functionality of the CRC [75]. As shown in Fig. 6b, they proposed a multilayered structure, in which the Ag and zinc oxide (ZnO)/PMMA layers are used as the solar reflective

layer and the silica-embedded perovskite nanocrystals layer on the top serves as the chromogenic layer. Unlike their previous work [71], the content of the perovskite nanocrystals in the chromogenic layer is relatively high so that the composite material itself can exhibit a certain color, thus achieving the function of color appearance in daytime. Meanwhile, the perovskite nanocrystals can effectively decrease the light-to-heat conversion by solar absorption owing to their photoluminescence behavior [76,77], which means that the solar heat absorbed by the chromogenic layer can be partially converted to photon and emit again, thus increasing the radiative cooling performance of the CRC in daytime. The fabricated

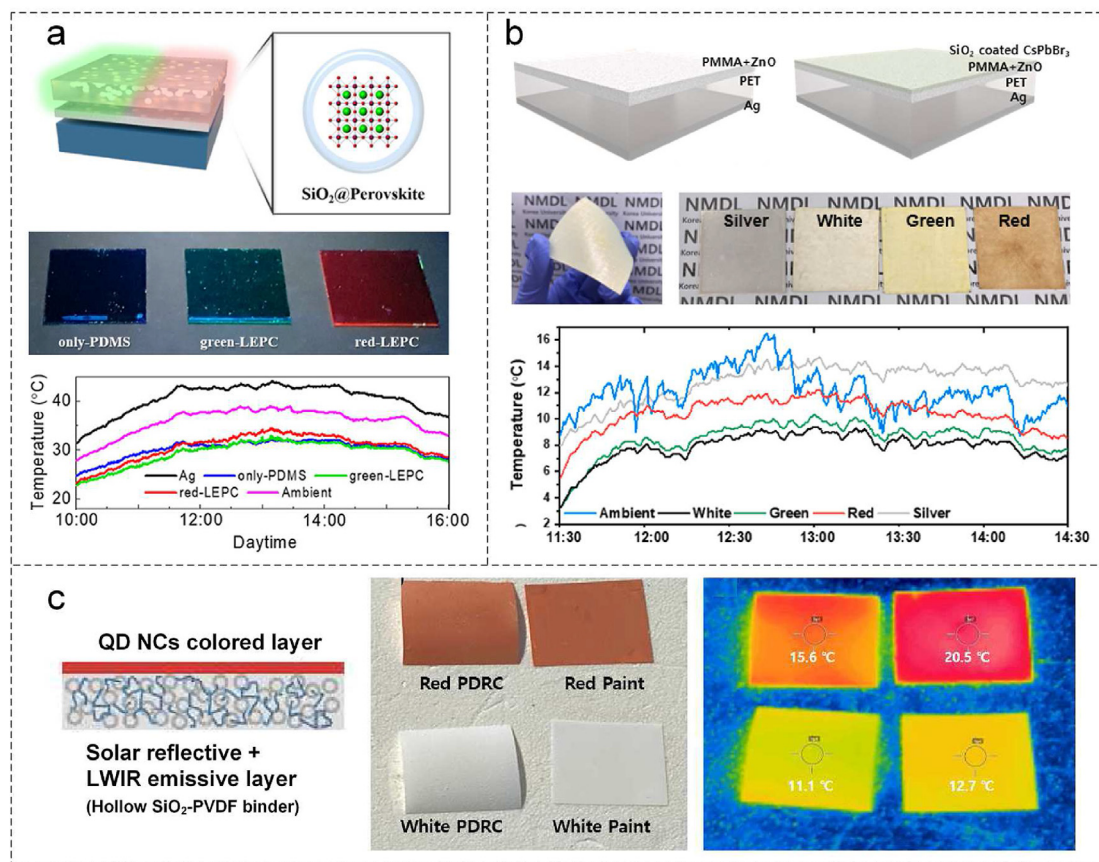


Fig. 6. a) The schematic and performances of the CRC [71]. b) Schematics and photographs of the CRC with and without the chromogenic layer, and their daytime radiative cooling performance [75]. c) CRCs and their surface temperature distribution [78]. CRC, colored radiative cooler.

CRCs with different colors can exhibit a subambient cooling temperature of 1.7–4.2 °C, which further proves the validity of the proposed structure. In order to improve the feasibility process and reduce processing costs of the CRC, in the next year, they proposed a new structure and technological process [78]. As shown in Fig. 6c, the CRC is composed of two functional layers, the chromogenic layer on the top and the solar reflective layer on the bottom. The colored radiative cooling function of the CRC follows the fundamental principle of their last work [75], i.e. the light-to-photon conversion of quantum dots in the chromogenic layer. What's more, they have made great improvements to the technological process. The reflective layer consists of hollow SiO₂ nanoparticles with high solar reflectivity and various polymer binders, which will be first dissolved in an organic solvent and then deposited in a target surface via spray coating. Then, the copper (Cu)-based quantum dots dissolved in chloroform can also be deposited on the reflective layer via spray coating on the reflective layer to generate different colors. The choice of these colloidal nanoparticle materials and spray processes enables the CRC to be low-cost, facile, and conducive to large-scale production. The results of the outdoor experiment demonstrated that the CRC can exhibit a 0.51–3.25 °C subambient temperature drop, and when compared to commercial coatings, the CRC can achieve a temperature drop of 5 °C.

The aforementioned works have proved that photoluminescence-based CRCs are effective in practical outdoor applications. But there is still a lack of research on the theoretical limit of their cooling power and color gamut range, which is important for identifying the performance bounds of photoluminescence-based CRCs. Facing with this problem, Min et al. investigated the radiative cooling

power limits of CRCs with different colors [79]. Based on the proposed design method of the linear-algebraic description of metamerism, they succeeded in demonstrating that the optimized wavelength photoluminescence conversion in the visible spectrum can enable the CRCs with any desired color in the entire absorptive color space while maintaining daytime subambient cooling performance. The optimized spectral characteristics are realized by photoluminescence colorants, which can be used as functional fillers to be combined with many existing nanoparticle-based radiative coolers to enhance their cooling and color performance [10,14,69,70]. In thermal calculation, the optimized photoluminescence colorant-based CRCs of highest-chroma red, green, and blue can achieve subambient steady-state temperatures, while the optimized non-photoluminescence colorant-based CRCs can only reach above-ambient temperatures. The temperature difference between these two kinds of coolers is greater than 9.5 K for all three colors, demonstrating the importance of introducing photoluminescence colorants into CRCs.

5.2. Nanoparticles-stacked CRC

In order to simplify the process for large-scale applications and improve the adaptability of CRCs to surfaces with different geometries, nanoparticles stacking has become an effective functional structure [80]. Bao et al. fabricated double-layer coatings for radiative cooling by using spraying coating methods [3]. The coatings are composed of a reflective TiO₂ particle layer and an emissive SiO₂ or SiC particle layer on the bottom, which has exhibited great radiative properties for radiative cooling. The TiO₂–SiO₂ coatings

have achieved 90.7% reflectivity in the solar spectrum and 90.11% emissivity with the atmospheric transparent window. In addition to exhibiting the intrinsic radiative properties of material particles, the nanoparticles-stacked structure with a rational particle size can exhibit different iridescent colors originating from the Bragg diffraction, showing great potential in CRCs [81,82].

In most colored radiative cooling research studies, the way of coloration by selective absorption has been served as a paradigm. However, this absorption-based coloration, anyhow, leads to the heating of the coolers, thus decreasing its cooling effect. To break this bottleneck, Lee et al. designed colloidal opals assemblies for colored radiative cooling based on the Bragg reflective coloration, which successfully gets rid of the limitations of the absorption-

based strategies [83]. As shown in Fig. 7a, the opals are assembled from SiO₂ colloidal nanospheres by a simple drop-casting process. Owing to the similarity between the size of the nanospheres and the wavelength of the visible light, the opals can be regarded as photonic crystals in the region. Hence, by adjusting the size of the nanospheres, the opals can exhibit different colors resulting from Bragg's diffraction instead of selective absorption [81,82]. The corresponding normal reflection spectra in Fig. 7b further support that these colors originate from a diffractive reflection. In addition, in the MIR spectrum, the opals will be converted to a homogenous medium due to their deep-subwavelength-scale property, which enhances heat emission in the atmospheric window. Thus, the opals feature the color

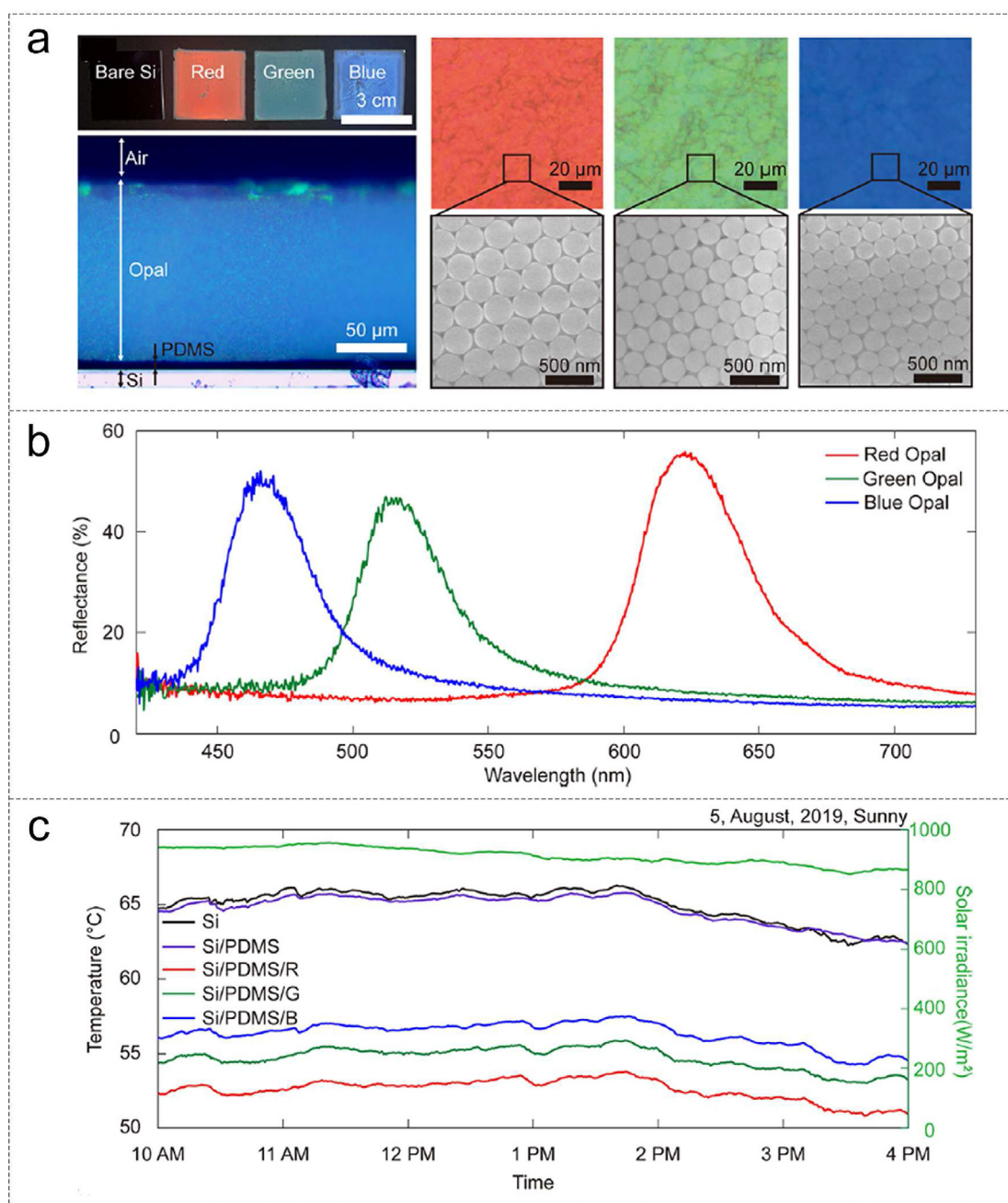


Fig. 7. a), b) Photographs and reflectivity of colloidal opals assemblies CRCs with different colors and SEM images of the reddish, greenish, and bluish opals. c) Radiative cooling performance of different CRCs under direct sunlight [83]. CRC, colored radiative cooler, SEM, scanning electron microscope.

preserving and radiative cooling effect, simultaneously. As shown in Fig. 7c, in the outdoor experiments, the opals effectively reduce the temperature of the substrate, c-Si, by as much as 13 °C, showing great potential in colored radiative cooling applications.

However, the above-mentioned nanoparticles-assembled CRCs rely on the use of monodisperse nanoparticles, which are challenging in cost-effective production. Taking a step forward, Zhu et al. demonstrated that a scalable and sustainable CRC can be realized by using cellulose nanocrystals as the raw material of a structurally colored film [84]. By coating cellulose nanocrystal films onto a porous, highly scattering ethylcellulose layer, a broadband

solar reflection and vibrant structural colors were achieved, simultaneously. Moreover, these CRCs can be manufactured by the commercial roll-to-roll process, which offers a low-cost and sustainable way to realize a daytime CRC.

6. Fibers-based CRC

Radiative cooling fibers for personal thermal management are an emerging topic, which have exhibited great potential for improving human comfort and energy saving for space heating/cooling [85,86]. When the targets go from artificial objects to

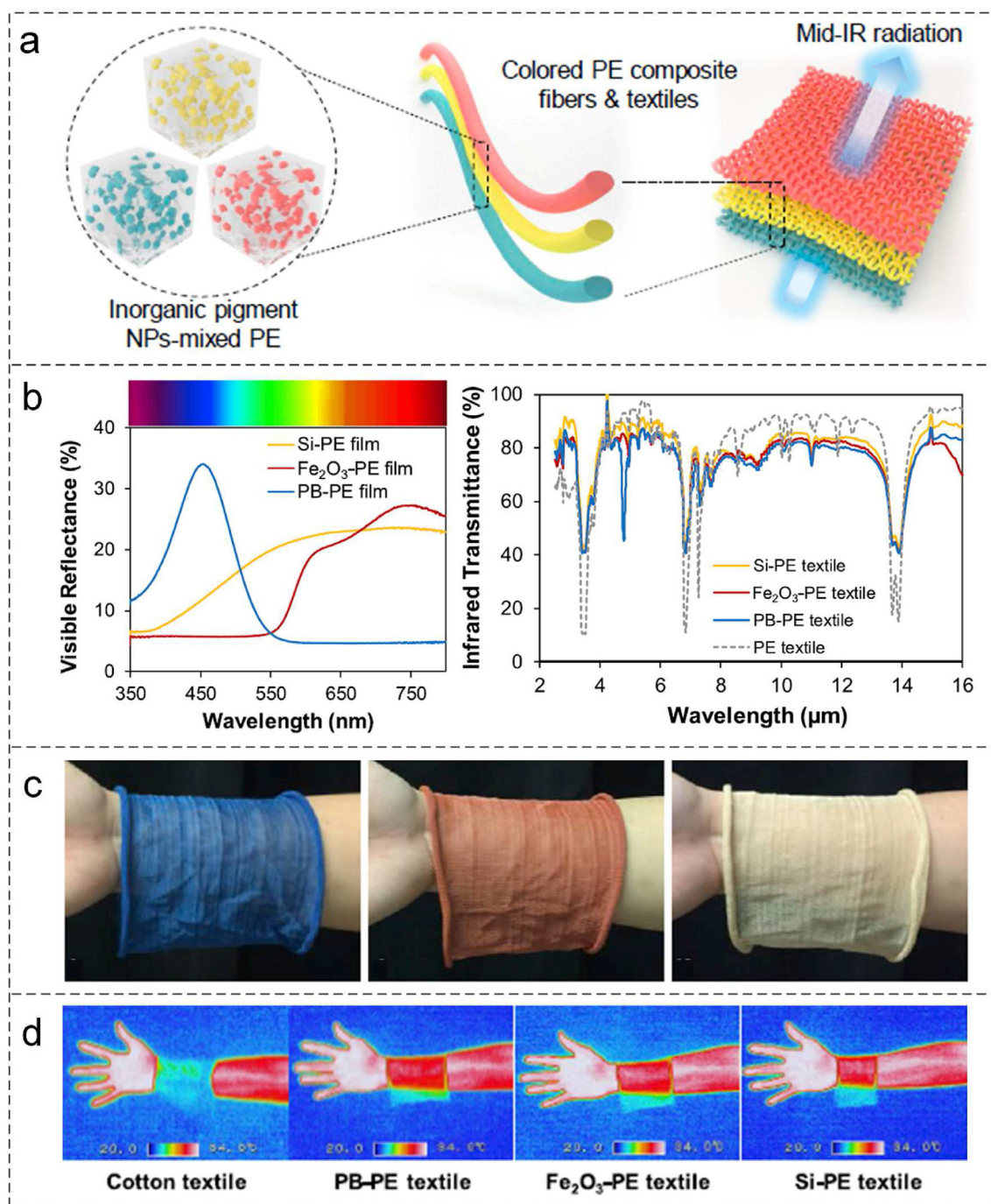



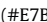










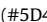



Fig. 8. Fiber-based CRCs: a) Design schematics. b) Visible reflectivity and MIR transmissivity. c) Photographs with good wearability. d) Infrared images of bare skin and skin covered by cotton and different CRCs [95]. CRC, colored radiative cooler; MIR, mid-infrared.

human beings, the radiative properties demands and base materials of CRCs are slightly different. In 2015, Chen et al. proposed an important concept of infrared-transparent visible-opaque fabric for personal thermal management [87]. Unlike the conventional radiative coolers with high emissivity, the infrared-transparent visible-opaque fabric is highly transparent in the MIR spectrum since the human skin is regarded as an ideal emitter ($\epsilon = 0.98$) [88]. From the perspective of the structure, the non-wearable radiative cooling

structures above are no longer applicable in personal thermal management. Inspired by a knitted sweater, the woven textile has been identified as an ideal candidate for its excellent air permeability and stretch properties [25]. Polymer materials such as polyethylene and polycaprolactam (nylon) stand out by the virtue of their high MIR transmissivity and plasticity, which make them easy to be processed into fibers and textiles. Further, by compounding light-scattering nanoparticles, such as air pores and ZnO,

Table 1
Representative compilation of key parameters and performances for CRCs.

CRC classification	Materials description	Subambient temperature values	Colors and their RGB color values in hexadecimal)	Manufacturing techniques	Year & Ref. No	
Photonic crystals	Ag-SiO ₂ -TiO ₂ multilayer	~10 K at noon when $T_{amb} = 298$ K, $h_c = 5$ W/(m ² ·K)	 (#FFF9FF)	/	2021 [46]	
	Si nanowires and quartz bars on Al substrate	Max. 18 K at noon when $T_{amb} = 300$ K, $h_c = 12$ W/(m ² ·K)	 (#FFCAC4)	/	2013 [53]	
	SiO ₂ -TiO ₂ multilayer	Avg. 4.4 K at noon	Transparent	Electron beam evaporation deposition	2022 [55]	
	Ag-SiO ₂ -Si ₃ N ₄ multilayer	Avg. 3.9 K at noon	 (#BCB55E), (#AA6971), (#4E8AB3)	Electron beam deposition, Plasma-enhanced chemical vapor deposition	2018 [56]	
	Ag-SiO ₂ -HfO ₂ multilayer with surface pattern	Avg. net cooling power = 37 W/m ² at noon	 (#E7B6BA), (#9DADEB), (#DCFFBF)	/	2020 [59]	
	Ag-SiO ₂ -SiN-MgF ₂ -SiC multilayer	Max. 6 K at noon when $T_{amb} = 303$ K, $h_c = 6$ W/(m ² ·K)	 (#FEE648), (#FD5BF2), (#00EAFB)	/	2019 [29]	
	Si-SiO ₂ -TiO ₂ multilayer	Do not fulfill subambient temperature at noon	 (#E379B6)	Electron beam deposition	2018 [63]	
	Ge-ZnS multilayer, polystyrene covered by Al foil, PDMS substrate	Avg. 3.5 K, Max. 6.9 K under 646 W/m ² solar irradiance	 (#8C1F1C), (#181616)	Magnetron sputtering	2023 [64]	
	Nanoparticles	Commercial paints with VDF-HFP or TiO ₂ /polymer composite	Max. 15.6 K at noon when $h_c = 5-7$ W/(m ² ·K)	 (#202123), (#2B51C0), (#FAEE0E), (#E34952)	Phase inversion	2020 [69]
		SiO ₂ core-Ag shell nanoparticles and plain Ag nanoparticles embedded in SiO ₂ and PDMS	Max. net cooling power = 114 W/m ² at noon	Wide color tunability by numerical calculation	/	2020 [70]
Ag deposited film, SiO ₂ coated CsPbX ₃ nanocrystals/PDMS composite		Avg. 6-7.4 K under ~700 W/m ² solar irradiance and $h_c = 8$ W/(m ² ·K)	 (#03A903), (#DF0E05)	Thermal evaporation, spin-coating	2020 [71]	
Phosphors with TiO ₂ /BaSO ₄ powders		Avg. 0.6-2.5 K	 (#A4B77D), (#A5C0A3), (#8DB7A3), (#D1A48F)	Scrape and bake	2022 [74]	
Ag and ZnO/PMMA, silica-embedded perovskite nanocrystals		Avg. 1.7-4.2 K under 900 W/m ² solar irradiance	 (#A7A19E), (#E0D7C4), (#DDD09A), (#CEA475)	Hot injection, sputtering, coating	2021 [75]	
Quantum dots, hollow SiO ₂ nanoparticles/polymer binder		Avg. 0.51-3.25 K under 886 W/m ² solar irradiance	 (#F9F6BF), (#A85E43)	Spray coating	2021 [78]	
Plasmonic sphere, SiO ₂ stacked microspheres		Avg. 1.9 K under ~881 W/m ² solar irradiance	 (#CFCACE), (#E0DDCE), (#D7D2CF), (#DDD9DA)	Sticking	2022 [80]	
Self-assembled silica opals on a Si wafer		Max. 15 K at daytime	 (#D86B55), (#4E818D), (#558AD7)	Solvent varying, solvent evaporation	2020 [83]	
CNC coated on porous EC-base layer		Avg. 1.4 K at noon under 900 W/m ² solar irradiation, max. 15.4 K at night	 (#5D4E90), (#83913A), (#B83453)	Blade-coating, roll-to-roll deposition	2022 [84]	
Fibers		Polyethylene	Provide sufficient cooling when $T_{amb} = 300$ K	Transparent	/	2015 [87]
	Inorganic pigment nanoparticles (Prussian blue, Fe ₂ O ₃ , Si) and Polyethylene	Avg. 1.7 K	 (#527EAC), (#C78E73), (#CDC1A3)	Mixed via compounding, extrusion	2019 [95]	

Note: '/' indicates that data is not shown in the reference. T_{amb} and h_c represent the ambient temperature and convective heat transfer coefficient, respectively. Max. and Avg. are the abbreviation for maximum and average, respectively. Abbreviations: CRC, colored radiative cooler; PDMS, polydimethylsiloxane; CNC, cellulose nanocrystal.

into the PE matrix fiber, the woven textiles can exhibit great radiative cooling performance even under direct sunlight due to their high solar reflectivity and MIR transmissivity [4].

In order to bring the radiative cooling technology into the wearable market, color control is an indispensable part as color selection is one of the most important factors in the wearable market [89]. However, owing to their high absorption in the MIR spectrum, the conventional organic dyes are unsuitable for fiber-based CRCs [90,91]. Therefore, the inorganic pigment nanoparticles have become ideal dyes in fiber-based CRCs for their nanoscale size, which have neglectable effect on the radiative properties of colored polymer mixtures in MIR wavelengths [92]. Additionally, on the basis of Mie theory, the dielectric or semiconductor with a high refractive index can achieve strong resonant light scattering within the visible spectrum by proper particle size regulation [93,94]. Thus, different colors can be obtained by controlling their nanoscale geometries. As shown in Fig. 8a and b, Cui et al. fabricated fiber-based CRCs by compounding inorganic pigment (Prussian blue, red iron oxide, or yellow silicon) nanoparticles into a PE matrix, which was then extruded into continuous and mechanically strong fibers for the knitting of colored textiles [95]. The diameter of these pigment nanoparticles ranges from 200 to 1,000 nm, which has little influence on the MIR transmissivity of PE while maintaining vivid colors. Additionally, with three primary color pigments, arbitrary colors can be obtained by mixing them in a proper ratio. The infrared images of the wrist covered by different fiber-based CRCs are shown in Fig. 8c and d. By efficiently transmitting human thermal radiation, the CRCs achieve a passive cooling effect of 1.6–1.8 °C compared with the cotton textile. The fiber-based CRCs set the foundation for radiative cooling technology in personal thermal management and make it closer to practical wearable applications.

7. Conclusions and prospects

Over few decades of development, radiative cooling technology has gradually become mature, whether in view of the cooling performance or the manufacturing process. However, there are still bottlenecks in the practical applications for its color deficiency. Faced with this problem, colored radiative cooling technology has attracted a lot of attention in recent years, and some outstanding research works have emerged. In this perspective paper, we give a review of the state-of-art CRCs with an emphasis on the emerging materials and strategies. Firstly, the basic physical concept of radiative cooling and colored radiative cooling is introduced, followed by the numerical fundamental principles for the performance of CRCs. Then, we investigate the relationship between the color appearance and the radiative cooling effect in CRCs and give our own strategy to balance these two indicators. Finally, based on the structure classification, CRCs can be mainly divided into three types, photonic crystal-based CRCs, nanoparticle-based CRCs, and fiber-based CRCs, which are discussed in detail in each section.

Table 1 collects the representative performance and key parameters from the above-mentioned research studies. It is seen that, similar to the traditional 'white' radiative coolers, CRCs have also shown remarkable daytime cooling abilities, although their vivid colors slightly hinder the maximal attainable cooling power. It is also worth noticing that the materials and manufacturing strategies are many and varied, which gives us a wide design freedom for fabricating colorful radiative coolers to meet the distinct application requirements. In general, all these emerging progresses of colored radiative cooling have advanced this concept and put it close to practical applications, significantly.

Here, we point out four potential directions to further promote the research, development, and applications of CRCs.

First, a machine learning algorithm is an efficient way to accelerate the structure optimization with a specific physical property, which has been widely applied in thermotics, optics, and mechanics [96–101]. By defining a specific property flag, the machine learning algorithm can quickly find the structure closest to the aimed property, even among a large number of candidates [102]. The structure design of CRCs is not an easy task since there are many variables affecting its cooling and color performance. For instance, the layer material types and distribution of multilayered CRCs and the particle types and geometries of nanoparticle-based CRCs are all important parameters in structural design, which makes it hard to find the optimal structure by manual or empirical filtering. In addition, in the future, the structural variables in CRCs can be further increased for a better colored radiative cooling effect, which makes it an arduous task to search the optimal structure. In this regard, by combining machine learning with radiative property calculation, the process of structural optimization can be effectively accelerated to achieve the ideal CRC design with a more complex structure and better performance. In this method, the most important is the definition of the property flag, which needs to balance the mutually restrictive relationship between color appearance and radiative cooling in a CRC.

Second, in many colored radiative cooling research studies, conventional pigments are widely used for color appearance due to their low cost and ease-of-processing. However, these pigments are not actually suitable for radiative cooling since their absorptivity in the UV and NIR spectrum sacrifices a huge radiative cooling power. The ideal pigment should exhibit highly selective absorption to reduce solar energy. In the past decade, highly selective absorption pigments have been investigated, including the pigments based on an dielectric film and TiO₂ nanoparticles by Smith et al. [103,104] and the studies on solar spectral optical properties of pigments by Levinson et al. [105,106]. Based on these inspirations, Chen et al. succeeded in enhancing the reflectivity of CRC in the NIR spectrum by replacing the commercial blue paint to a Sudan blue colorant, thus further improving the radiative cooling effect [69]. Nevertheless, these pigments still suffer from poor efficiency, color distortion, or UV absorption, which blocks their application in CRCs. Hence, the ideal selective pigment, which maximizes its reflectivity in the UV and NIR spectrum while maintaining a vivid color, is eagerly in demand.

Third, in addition to radiative coolers with vivid colors, the efforts on developing visibly transparent radiative coolers (VTRCs) are booming recently [107,108]. Broadly speaking, transparency is also a kind of color and is highly demanded in the radiative cooling applications toward transparent objects, such as the windows of buildings and vehicles, and coatings that preserve the original colors of objects. An idea VTRC should feature high visible light transparency, high NIR reflectance, as well as high emissivity within the atmospheric window, simultaneously. The function of visibly transparent but NIR reflective can be realized by two means: i) wide bandgaps semiconductors, such as indium tin oxide and fluorine-doped tin oxide [109]; ii) dielectric-metal-dielectric composite structures, such as ZnO/Ag/ZnO and TiO₂/Cu/TiO₂ [110–112]. The transparent emitters are mainly made of organic polymers, such as PMMA, polycarbonate, and ethylene-vinyl acetate [113,114]. For instance, Jin et al. reported on a VTRC window by combining a multilayer stack of Ag–SiO₂ and a uniform layer of PDMS, which achieved high visible transparency (>60%), IR reflectivity (>89%), and thermal emissivity (>95%). Consequently, this window can lower the interior temperature by as much as 7 °C [115]. Despite the significant progress, achieving high visible transmission always accompanies the considerable sacrifice of a high NIR reflection or high thermal emissivity. Therefore, there is still a long way to go before a perfect VTRC is developed.

Last but not least, for colored radiative cooling, as a technology facing the consumer market, besides its functional performance, its reliability in practical application is also very important. Recently, many CRCs with good performance actually face various reliability problems in real application scenarios. For the metal-based CRCs, the metal materials are easy to be oxidized and fail in the air, and in the outdoor applications, rain seepage will also accelerate the corrosion of metal [116]. Moreover, the surface pollution of a CRC will also bring great challenges to its practical applications. The attachment of dust pollutants in the outdoor environment will destroy the selective reflectivity of the CRC in the solar wavelength [117]. The reliability research of traditional 'white' radiative cooler has been advanced in recent years, including wear resistance, hydrophobicity [118], corrosion resistance, fire resistance [119], and radiative cooling performance of materials in different weathers [120]. However, there are few research studies on the reliability of CRCs. Compared with a traditional 'white' radiative cooler, CRCs have more stringent requirements on reliability because in addition to the requirements of radiative cooling, there are also requirements on color appearance, which makes the study of the reliability mechanism more complicated. Recently, Liu et al. reported on a colored ZrO₂-PVDF bilayer coating with subambient radiative cooling performance, self-cleaning, and weather-resistance properties [121]. Apart from the subambient temperature drop of about 3 °C, these red bilayer CRC coatings demonstrate prominent anti-blots properties after water scouring since the low surface energy substance, PVDF, endows the super-hydrophobicity with a water contact angle of above 150°. This reminds us that the reliability of CRCs can be divided into two key points, one is the self-cleaning of the radiative cooling component and the other is the preservation of the colored structure. The former requirement is just the same as a traditional radiative cooler, and the latter can be achieved by providing extra encapsulation strategies. Take a photoluminescent nanocrystals-based color layer as an example, coating an extra silica protective layer onto the nanocrystal surface, the oxygen/moisture resistance of these colored nanoparticles can be enhanced; thus, improving their stability under harsh outdoor environments [122]. Overall, reliability is definitely a crucial issue on the road to the practical application of CRCs, which is a virgin land worth exploring.

CRedit author statement

Xie Bin: conceptualization and writing-review & editing. **Liu Yida:** conceptualization, data curation and writing-original draft. **Xi Wang:** visualization and formal analysis. **Hu Run:** conceptualization, resources and supervision.

Declaration of competing interest

The authors declare that they have no known competing financial interests or personal relationships that could have appeared to influence the work reported in this paper.

Data availability

No data was used for the research described in the article.

Acknowledgments

This work was supported by the National Natural Science Foundation of China (52211540005, 52106089, 52076087) National Key R&D Program from Ministry of Science and Technology of China (2022YFA1203100), Wuhan City Science and Technology Program (2020010601012197), the Open Project Program of Wuhan

National Laboratory for Optoelectronics (2021WNLOKF004), Wuhan Knowledge Innovation Shuguang Program, and Science and Technology Program of Hubei Province (2021BLB176). B.X. and Y.L. contributed equally.

References

- [1] S. Catalanotti, V. Cuomo, G. Piro, D. Ruggi, V. Silvestrini, G. Troise, The radiative cooling of selective surfaces, *Sol. Energy* 17 (1975) 83–89, [https://doi.org/10.1016/0038-092X\(75\)90062-6](https://doi.org/10.1016/0038-092X(75)90062-6).
- [2] S. Atiganyanun, J.B. Plumley, S.J. Han, K. Hsu, J. Cytrynbaum, T.L. Peng, S.M. Han, S.E. Han, Effective radiative cooling by paint-format microsphere-based photonic random media, *ACS Photonics* 5 (2018) 1181–1187, <https://doi.org/10.1021/acsp Photonics.7b01492>.
- [3] H. Bao, C. Yan, B. Wang, X. Fang, C.Y. Zhao, X. Ruan, Double-layer nanoparticle-based coatings for efficient terrestrial radiative cooling, *Sol. Energy Mater. Sol. Cells* 168 (2017) 78–84, <https://doi.org/10.1016/j.solmat.2017.04.020>.
- [4] L. Cai, A.Y. Song, W. Li, P.C. Hsu, D. Lin, P.B. Catrysse, Y. Liu, Y. Peng, J. Chen, H. Wang, J. Xu, A. Yang, S. Fan, Y. Cui, Spectrally selective nanocomposite textile for outdoor personal cooling, *Adv. Mater.* 30 (2018), 1802152, <https://doi.org/10.1002/adma.201802152>.
- [5] Z. Chen, L. Zhu, A. Raman, S. Fan, Radiative cooling to deep sub-freezing temperatures through a 24-h day-night cycle, *Nat. Commun.* 7 (2016), 13729, <https://doi.org/10.1038/ncomms13729>.
- [6] M.M. Hossain, B. Jia, M. Gu, A metamaterial emitter for highly efficient radiative cooling, *Adv. Opt. Mater.* 3 (2015) 1047–1051, <https://doi.org/10.1002/adom.201500119>.
- [7] P.-C. Hsu, A.Y. Song, P.B. Catrysse, C. Liu, Y. Peng, J. Xie, S. Fan, Y. Cui, Radiative human body cooling by nanoporous polyethylene textile, *Science* 353 (2016) 1019–1023, <https://doi.org/10.1126/science.aaf5471>.
- [8] R. He, Y. Liao, J. Huang, T. Cheng, X. Zhang, P. Yang, H. Liu, K. Liu, Radiant air-conditioning with infrared transparent polyethylene aerogel, *Mater. Today Energy* 21 (2021), 100800, <https://doi.org/10.1016/j.mtener.2021.100800>.
- [9] J. Kou, Z. Jurado, Z. Chen, S. Fan, A.J. Minnich, Daytime radiative cooling using near-black infrared emitters, *ACS Photonics* 4 (2017) 626–630, <https://doi.org/10.1021/acsp Photonics.6b00991>.
- [10] J. Mandal, Y. Fu, A.C. Overvig, M. Jia, K. Sun, N.N. Shi, H. Zhou, X. Xiao, N. Yu, Y. Yang, Hierarchically porous polymer coatings for highly efficient passive daytime radiative cooling, *Science* 362 (2018) 315–319, <https://doi.org/10.1126/science.aat9513>.
- [11] A.P. Raman, M.A. Anoma, L. Zhu, E. Rephaeli, S. Fan, Passive radiative cooling below ambient air temperature under direct sunlight, *Nature* 515 (2014) 540–544, <https://doi.org/10.1038/nature13883>.
- [12] E. Rephaeli, A. Raman, S. Fan, Ultrabroadband photonic structures to achieve high-performance daytime radiative cooling, *Nano Lett.* 13 (2013) 1457–1461, <https://doi.org/10.1021/nl4004283>.
- [13] D. Miao, X. Wang, J. Yu, B. Ding, Nanoengineered textiles for outdoor personal cooling and drying, *Adv. Funct. Mater.* 32 (2022), 2209029, <https://doi.org/10.1002/adfm.202209029>.
- [14] Y. Zhai, Y. Ma, S.N. David, D. Zhao, R. Lou, G. Tan, R. Yang, X. Yin, Scalable-manufactured randomized glass-polymer hybrid metamaterial for daytime radiative cooling, *Science* 355 (2017) 1062–1066, <https://doi.org/10.1126/science.aai7899>.
- [15] Y. Chan, Y. Zhang, T. Tennakoon, S.C. Fu, K.C. Chan, C.Y. Tso, K.M. Yu, M.P. Wan, B.L. Huang, S. Yao, H. Qiu, C.Y.H. Chao, Potential passive cooling methods based on radiation controls in buildings, *Energy Convers. Manag.* 272 (2022), 116342, <https://doi.org/10.1016/j.enconman.2022.116342>.
- [16] X. Yin, R. Yang, G. Tan, S. Fan, Terrestrial radiative cooling: using the cold universe as a renewable and sustainable energy source, *Science* 370 (2020) 786–791, <https://doi.org/10.1126/science.abb0971>.
- [17] T. Li, Y. Zhai, S. He, W. Gan, Z. Wei, M. Heidarinejad, D. Dalgo, R. Mi, X. Zhao, J. Song, J. Dai, C. Chen, A. Aili, A. Vellore, A. Martini, R. Yang, J. Srebric, X. Yin, L. Hu, A radiative cooling structural materials, *Science* 364 (2019) 760–763, <https://doi.org/10.1126/science.aau9101>.
- [18] J. Chai, J. Fan, Advanced thermal regulating materials and systems for energy saving and thermal comfort in buildings, *Mater. Today Energy* 24 (2022), 100925, <https://doi.org/10.1016/j.mtener.2021.100925>.
- [19] S. Son, Y. Liu, D. Chae, H. Lee, Cross-linked porous polymeric coating without a metal-reflective layer for sub-ambient radiative cooling, *ACS Appl. Mater. Interfaces* 12 (2020) 57832–57839, <https://doi.org/10.1021/acsaami.0c14792>.
- [20] L. Chen, K. Zhang, M. Ma, S. Tang, F. Li, X. Niu, Sub-ambient radiative cooling and its application in buildings, *Build. Simul.* 13 (2020) 1165–1189, <https://doi.org/10.1007/s12273-020-0646-x>.
- [21] X. Lu, P. Xu, H. Wang, T. Yang, J. Hou, Cooling potential and applications prospects of passive radiative cooling in buildings: the current state-of-the-art, *Renew. Sustain. Energy Rev.* 65 (2016) 1079–1097, <https://doi.org/10.1016/j.rser.2016.07.058>.
- [22] T. Hoyt, E. Arens, H. Zhang, Extending air temperature setpoints: simulated energy savings and design considerations for new and retrofit buildings, *Build. Environ.* 88 (2015) 89–96, <https://doi.org/10.1016/j.buildenv.2014.09.010>.

- [23] A. Sunawar, I. Garniwa, C. Hudaya, The characteristics of heat inside a parked car as energy source for thermoelectric generators, *Int. J. Energy Environ. Eng.* 10 (2019) 347–356, <https://doi.org/10.1007/s40095-019-0311-2>.
- [24] Y. Zhao, W. Yi, A.P.C. Chan, F.K.W. Wong, M.C.H. Yam, Evaluating the physiological and perceptual responses of wearing a newly designed cooling vest for construction workers, *Ann. Work Expo. Health* 61 (2017) 883–901, <https://doi.org/10.1093/annweh/wxx055>.
- [25] R. Hu, Y. Liu, S. Shin, S. Huang, X. Ren, W. Shu, J. Cheng, G. Tao, W. Xu, R. Chen, X. Luo, Emerging materials and strategies for personal thermal management, *Adv. Energy Mater.* 10 (2020), 1903921, <https://doi.org/10.1002/aenm.201903921>.
- [26] A. Berk, G.P. Anderson, P.K. Acharya, L.S. Bernstein, L. Muratov, J. Lee, M. Fox, S.M. Adler-Golden, J.H. Chetwynd Jr., M.L. Hoke, R.B. Lockwood, J.A. Gardner, T.W. Cooley, C.C. Borel, P.E. Lewis, E.P. Shettle, MODTRAN™ 5: 2006 update, *Proc. SPIE* 6233 (2006) 62331F, <https://doi.org/10.1117/12.665077>.
- [27] B. Zhao, M. Hu, X. Ao, Q. Xuan, G. Pei, Comprehensive photonic approach for diurnal photovoltaic and nocturnal radiative cooling, *Sol. Energy Mater. Sol. Cells* 178 (2018) 266–272, <https://doi.org/10.1016/j.solmat.2018.01.023>.
- [28] B. Zhao, M. Hu, X. Ao, N. Chen, G. Pei, Radiative cooling: a review of fundamentals, materials, applications, and prospects, *Appl. Energy* 236 (2019) 489–513, <https://doi.org/10.1016/j.apenergy.2018.12.018>.
- [29] C. Sheng, Y. An, J. Du, X. Li, Colored radiative cooler under optical Tamm resonance, *ACS Photonics* 6 (2019) 2545–2552, <https://doi.org/10.1021/acsp Photonics.9b01005>.
- [30] S.A. Mikaeva, A.S. Mikaeva, O.E. Zheleznikova, *Glass Ceram.* 72 (2016) 387–389, <https://doi.org/10.1007/s10717-016-9795-x>.
- [31] G. Chen, J. Damasco, H. Qiu, W. Shao, T.Y. Ohulchanskyy, R.R. Valiev, X. Wu, G. Han, Y. Wang, C. Yang, H. Agren, P.N. Prasad, Energy-cascaded upconversion in an organic dye-sensitized core/shell fluoride nanocrystal, *Nano Lett.* 15 (2015) 7400–7407, <https://doi.org/10.1021/acs.nanolett.5b02830>.
- [32] W. Zou, C. Visser, J.A. Maduro, M.S. Pshenichnikov, J.C. Hummelen, Broadband dye-sensitized upconversion of near-infrared light, *Nat. Photonics* 6 (2012) 560–564, <https://doi.org/10.1038/nphoton.2012.158>.
- [33] N. Li, S. Oida, G.S. Tulevski, S.J. Han, J.B. Hannon, D.K. Sadana, T.C. Chen, Efficient and bright organic light-emitting diodes on single-layer graphene electrodes, *Nat. Commun.* 4 (2013) 2294, <https://doi.org/10.1038/ncomms3294>.
- [34] W.H. Koo, S.M. Jeong, F. Araoka, K. Ishikawa, S. Nishimura, T. Toyooka, H. Takezoe, Light extraction from organic light-emitting diodes enhanced by spontaneously formed buckles, *Nat. Photonics* 4 (2010) 222–226, <https://doi.org/10.1038/nphoton.2010.7>.
- [35] M. Kneissl, T.-Y. Seong, J. Han, H. Amano, The emergence and prospects of deep-ultraviolet light-emitting diode technologies, *Nat. Photonics* 13 (2019) 233–244, <https://doi.org/10.1038/s41566-019-0359-9>.
- [36] G. Xing, B. Wu, X. Wu, M. Li, B. Du, Q. Wei, J. Guo, E.K. Yeow, T.C. Sum, W. Huang, Transcending the slow bimolecular recombination in lead-halide perovskites for electroluminescence, *Nat. Commun.* 8 (2017), 14558, <https://doi.org/10.1038/ncomms14558>.
- [37] S. Hirata, Y. Sakai, K. Masui, H. Tanaka, S.Y. Lee, H. Nomura, N. Nakamura, M. Yasumatsu, H. Nakanotani, Q. Zhang, K. Shizu, H. Miyazaki, C. Adachi, Highly efficient blue electroluminescence based on thermally activated delayed fluorescence, *Nat. Mater.* 14 (2015) 330–336, <https://doi.org/10.1038/nmat4154>.
- [38] R.S. Sundaram, M. Engel, A. Lombardo, R. Krupke, A.C. Ferrari, P. Avouris, M. Steiner, Electroluminescence in single layer MoS₂, *Nano Lett.* 13 (2013) 1416–1421, <https://doi.org/10.1021/nl400516a>.
- [39] J.M. Richter, M. Abdi-Jalebi, A. Sadhanala, M. Tabachnyk, J.P.H. Rivett, L.M. Pazos-Outon, K.C. Godel, M. Price, F. Deschler, R.H. Friend, Enhancing photoluminescence yields in lead halide perovskites by photon recycling and light out-coupling, *Nat. Commun.* 7 (2016), 13941, <https://doi.org/10.1038/ncomms13941>.
- [40] A. Splendiani, L. Sun, Y. Zhang, T. Li, J. Kim, C.Y. Chim, G. Galli, F. Wang, Emerging photoluminescence in monolayer MoS₂, *Nano Lett.* 10 (2010) 1271–1275, <https://doi.org/10.1021/nl903868w>.
- [41] D.L. Monika, H. Nagabhushana, S.C. Sharma, B.M. Nagabhushana, R. Hari Krishna, Synthesis of multicolor emitting Sr_{2-x}Sm_xCeO₄ nanophosphor with compositionally tuneable photo and thermoluminescence, *Chem. Eng. J.* 253 (2014) 155–164, <https://doi.org/10.1016/j.cej.2014.05.028>.
- [42] H. Guo, Y. Wang, G. Li, J. Liu, P. Peng, D. Liu, Cyan emissive super-persistent luminescence and thermoluminescence in BaZrSi₃O₉:Eu²⁺, Pr³⁺ phosphors, *J. Mater. Chem. C* 5 (2017) 2844–2851, <https://doi.org/10.1039/C7TC00133A>.
- [43] K. Baek, Y. Kim, S. Mohd-Noor, J.K. Hyun, Mie resonant structural colors, *ACS Appl. Mater. Interfaces* 12 (2020) 5300–5318, <https://doi.org/10.1021/acsnano.9b16683>.
- [44] H.S. Fairman, M.H. Brill, H. Hemmendinger, How the CIE 1931 color-matching functions were derived from Wright-Guild data, *Color Res. Appl.* 22 (1997) 11–23, [https://doi.org/10.1002/\(SICI\)1520-6378\(199702\)22:1<11::AID-COLA>3.3.CO;2-F](https://doi.org/10.1002/(SICI)1520-6378(199702)22:1<11::AID-COLA>3.3.CO;2-F).
- [45] J. Schanda, *Colorimetry: Understanding the CIE System*, John Wiley & Sons, New Jersey, USA, 2007.
- [46] X. Wang, Y. Liu, W. Zhao, R. Hu, X. Luo, Colored radiative cooling: how to balance color display and radiative cooling performance, *Int. J. Therm. Sci.* 170 (2021), 107172, <https://doi.org/10.1016/j.ijthermalsci.2021.107172>.
- [47] W. Li, S. Fan, Nanophotonic control of thermal radiation for energy applications, *Opt. Express* 26 (2018) 15995–16021, <https://doi.org/10.1364/OE.26.015995>.
- [48] K. Feng, Q. Li, J. Liu, P. Guan, J. Yuan, G. Cai, N. Chen, Y. Bu, Symmetric thin films based on silicon materials for angle-insensitive full-color structural colors, *Adv. Mater. Technol.* 8 (2023), 2200529, <https://doi.org/10.1002/admt.202200529>.
- [49] Y. Cui, Y. He, Y. Jin, F. Ding, L. Yang, Y. Ye, S. Zhong, Y. Lin, S. He, Plasmonic and metamaterial structures as electromagnetic absorbers, *Laser Photon. Rev.* 8 (2014) 495–520, <https://doi.org/10.1002/lpor.201400026>.
- [50] Y. Cui, K.H. Fung, J. Xu, H. Ma, Y. Jin, S. He, N.X. Fang, Ultrabroadband light absorption by a sawtooth anisotropic metamaterial slab, *Nano Lett.* 12 (2012) 1443–1447, <https://doi.org/10.1021/nl204118h>.
- [51] Y. Li, W. Gao, L. Li, L. Guo, H. Ge, R. Xie, H. Wang, F. Wang, B. An, Ultrabroadband thermal radiator for daytime passive radiative cooling based on single dielectric SiO₂ on metal Ag, *Energy Rep.* 8 (2022) 852–859, <https://doi.org/10.1016/j.egy.2021.12.026>.
- [52] G.J. Lee, D. Kim, S.Y. Heo, Y.M. Song, Spectrally and spatially selective emitters using polymer hybrid spoof plasmonics, *ACS Appl. Mater. Interfaces* 12 (2020) 53206–53214, <https://doi.org/10.1021/acsnano.1c13177>.
- [53] L. Zhu, A. Raman, S. Fan, Color-preserving daytime radiative cooling, *Appl. Phys. Lett.* 103 (2013), 223902, <https://doi.org/10.1063/1.4835995>.
- [54] L. Cao, P. Fan, E.S. Barnard, A.M. Brown, M.L. Brongersma, Tuning the color of silicon nanostructures, *Nano Lett.* 10 (2010) 2649–2654, <https://doi.org/10.1021/nl1013794>.
- [55] Y. Zhu, H. Luo, C. Yang, B. Qin, P. Ghosh, S. Kaur, W. Shen, M. Qiu, P. Belov, Q. Li, Color-preserving passive radiative cooling for an actively temperature-regulated enclosure, *Light Sci. Appl.* 11 (2022) 122, <https://doi.org/10.1038/s41377-022-00810-y>.
- [56] G.J. Lee, Y.J. Kim, H.M. Kim, Y.J. Yoo, Y.M. Song, Colored, daytime radiative coolers with thin-film resonators for aesthetic purposes, *Adv. Opt. Mater.* 6 (2018), 1800707, <https://doi.org/10.1002/adom.201800707>.
- [57] E. Blandre, M. Shimizu, A. Kohiyama, H. Yugami, P.-O. Chapuis, R. Vaillon, Spectrally shaping high-temperature radiators for thermophotovoltaics using Mo-HfO₂ trilayer-on-substrate structures, *Opt. Express* 26 (2018) 4346–4357, <https://doi.org/10.1364/OE.26.004346>.
- [58] E. Blandre, P.-O. Chapuis, R. Vaillon, Spectral and total temperature-dependent emissivities of few-layer structures on a metallic substrate, *Opt. Express* 24 (2016) A374–A384, <https://doi.org/10.1364/OE.24.00A374>.
- [59] E. Blandre, R.A. Yalcin, K. Joulain, J. Dreviron, Microstructured surfaces for colored and non-colored sky radiative cooling, *Opt. Express* 28 (2020) 29703–29713, <https://doi.org/10.1364/OE.401368>.
- [60] Z.-Y. Yang, S. Ishii, T. Yokoyama, T.D. Dao, M.-G. Sun, P.S. Pankin, I.V. Timofeev, T. Nagao, K.-P. Chen, Narrowband wavelength selective thermal emitters by confined Tamm plasmon polaritons, *ACS Photonics* 4 (2017) 2212–2219, <https://doi.org/10.1021/acsp Photonics.7b00408>.
- [61] R. Li, C. Zhang, X. Li, Schottky hot-electron photodetector by cavity-enhanced optical Tamm resonance, *Appl. Phys. Lett.* 110 (2017), 013902, <https://doi.org/10.1063/1.4973644>.
- [62] C. Zhang, K. Wu, V. Giannini, X. Li, Planar hot-electron photodetection with Tamm plasmons, *ACS Nano* 11 (2017) 1719–1727, <https://doi.org/10.1021/acsnano.6b07578>.
- [63] W. Li, Y. Shi, Z. Chen, S. Fan, Photonic thermal management of coloured objects, *Nat. Commun.* 9 (2018) 4240, <https://doi.org/10.1038/s41467-018-06535-0>.
- [64] S. Jeon, S. Son, S. Min, H. Park, H. Lee, J. Shin, Daylong sub-ambient radiative cooling with full-color exterior based on thermal radiation and solar decoupling, *Adv. Opt. Mater.* 11 (2023), 2202129, <https://doi.org/10.1002/adom.202202129>.
- [65] H.E. Türeci, L. Ge, S. Rotter, A.D. Stone, Strong interactions in multimode random lasers, *Science* 320 (2008) 643–646, <https://doi.org/10.1126/science.1155311>.
- [66] D.S. Wiersma, The physics and applications of random lasers, *Nat. Phys.* 4 (2008) 359–367, <https://doi.org/10.1038/nphys971>.
- [67] M.F. Weber, C.A. Stover, L.R. Gilbert, T.J. Nevitt, A.J. Ouderkerk, Giant birefringent optics in multilayer polymer mirrors, *Science* 287 (2000) 2451–2456, <https://doi.org/10.1126/science.287.5462.2451>.
- [68] S.D. Hart, G.R. Maskaly, B. Temelkuran, P.H. Pridoux, J.D. Joannopoulos, Y. Fink, External reflection from omnidirectional dielectric inorganic fibers, *Science* 296 (2002) 510–513, <https://doi.org/10.1126/science.1070050>.
- [69] Y. Chen, J. Mandal, W. Li, A. Smith-Washington, C.-C. Tsai, W. Huang, S. Shrestha, N. Yu, R.P.S. Han, A. Cao, Y. Yang, Colored and paintable bilayer coatings with high solar-infrared reflectance for efficient cooling, *Sci. Adv.* 6 (2020), eaaz5413, <https://doi.org/10.1126/sciadv.aaz5413>.
- [70] R.A. Yalcin, E. Blandre, K. Joulain, J. Dreviron, Colored radiative cooling coatings with nanoparticles, *ACS Photonics* 7 (2020) 1312–1322, <https://doi.org/10.1021/acsp Photonics.0c00513>.
- [71] S. Jeon, S. Son, S.Y. Lee, D. Chae, J.H. Bae, H. Lee, S.J. Oh, Multifunctional daytime radiative cooling devices with simultaneous light-emitting and radiative cooling functional layers, *ACS Appl. Mater. Interfaces* 12 (2020) 54763–54772, <https://doi.org/10.1021/acsnano.1c16241>.
- [72] M.V. Kovalenko, L. Protesescu, M.I. Bodnarchuk, Properties and potential optoelectronic applications of lead halide perovskite nanocrystals, *Science* 358 (2017) 745–750, <https://doi.org/10.1126/science.aam7093>.
- [73] S. Jeon, M.C. Jung, J. Ahn, H.K. Woo, J. Bang, D. Kim, S.Y. Lee, H.Y. Woo, J. Jeon, M.J. Han, T. Paik, S.J. Oh, Post-synthetic oriented attachment of CsPbBr₃ perovskite nanocrystal building blocks: from first principle calculation to

- experimental demonstration of size and dimensionality (0D/1D/2D), *Nano-scale Horiz.* 5 (2020) 960–970. <https://doi.org/10.1039/d0nh00029a>.
- [74] J. Xu, R. Wan, W. Xu, Z. Ma, X. Cheng, R. Yang, X. Yin, Colored radiative cooling coatings using phosphor dyes, *Mater. Today Nano* 19 (2022), 100239, <https://doi.org/10.1016/j.mtnano.2022.100239>.
- [75] S. Son, S. Jeon, D. Chae, S.Y. Lee, Y. Liu, H. Lim, S.J. Oh, H. Lee, Colored emitters with silica-embedded perovskite nanocrystals for efficient daytime radiative cooling, *Nano Energy* 79 (2021), 105461. <https://doi.org/10.1016/j.nanoen.2020.105461>.
- [76] Y. Dong, Y. Gu, Y. Zou, J. Song, L. Xu, J. Li, J. Xue, X. Li, H. Zeng, Improving all-inorganic perovskite photodetectors by preferred orientation and plasmonic effect, *Small* 12 (2016) 5622–5632. <https://doi.org/10.1002/sml.201602366>.
- [77] J. Kang, L.W. Wang, High defect tolerance in lead halide perovskite CsPbBr₃, *J. Phys. Chem. Lett.* 8 (2017) 489–493, <https://doi.org/10.1021/acs.jpcl.7b02800>.
- [78] T.Y. Yoon, S. Son, S. Min, D. Chae, H.Y. Woo, J.-Y. Chae, H. Lim, J. Shin, T. Paik, H. Lee, Colloidal deposition of colored daytime radiative cooling films using nanoparticle-based inks, *Mater. Today Phys.* 21 (2021), 100510, <https://doi.org/10.1016/j.mtphys.2021.100510>.
- [79] S. Min, S. Jeon, K. Yun, J. Shin, All-color sub-ambient radiative cooling based on photoluminescence, *ACS Photonics* 9 (2022) 1196–1205, <https://doi.org/10.1021/acsp.2c01648>.
- [80] M. Chen, D. Pang, H. Yan, Colored passive daytime radiative cooling coatings based on dielectric and plasmonic spheres, *Appl. Therm. Eng.* 216 (2022), 119125, <https://doi.org/10.1016/j.applthermaleng.2022.119125>.
- [81] S.-H. Kim, S.-J. Jeon, W.C. Jeong, H.S. Park, S.-M. Yang, Optofluidic synthesis of electroresponsive photonic Janus balls with isotropic structural colors, *Adv. Mater.* 20 (2008) 4129–4134. <https://doi.org/10.1002/adma.200801167>.
- [82] Q. Zhao, C.E. Finlayson, D.R. Snoswell, A. Haines, C. Schafer, P. Spahn, G.P. Hellmann, A.V. Petukhov, L. Herrmann, P. Burdet, P.A. Midgley, S. Butler, M. Mackley, Q. Guo, J.J. Baumberg, Large-scale ordering of nanoparticles using viscoelastic shear processing, *Nat. Commun.* 7 (2016), 11661, <https://doi.org/10.1038/ncomms11661>.
- [83] H.H. Kim, E. Im, S. Lee, Colloidal photonic assemblies for colorful radiative cooling, *Langmuir* 36 (2020) 6589–6596, <https://doi.org/10.1021/acs.langmuir.0c00051>.
- [84] W. Zhu, B. Drogue, Q. Shen, Y. Zhang, T.G. Parton, X. Shan, R.M. Parker, M.F.L. De Volder, T. Deng, S. Vignolini, T. Li, Structurally colored radiative cooling cellulosic films, *Adv. Sci.* 9 (2022), 2202061, <https://doi.org/10.1002/advs.202202061>.
- [85] Office of Energy Efficiency and Renewable Energy, 2011 Buildings Energy Data Book, March, 2011. <https://ieer.org/resource/energy-issues/2011-buildings-energy-data-book>.
- [86] P.-C. Hsu, X. Li, Photon-engineered radiative cooling textiles, *Science* 370 (2020) 784–785. <https://doi.org/10.1126/science.abe4476>.
- [87] J.K. Tong, X. Huang, S.V. Boriskina, J. Loomis, Y. Xu, G. Chen, Infrared-transparent visible-opaque fabrics for wearable personal thermal management, *ACS Photonics* 2 (2015) 769–778, <https://doi.org/10.1021/acsp.5b00140>.
- [88] J. Steketee, Spectral emissivity of skin and pericardium, *Phys. Med. Biol.* 18 (1973) 686. <https://doi.org/10.1088/0031-9155/18/5/307>.
- [89] S.G. Marshall, H.O. Jackson, M.S. Stanley, M. Kefgen, P. Touchie-Specht, *Individuality in Clothing Selection and Personal Appearance*, Pearson Prentice Hall, Upper Saddle River, NJ, USA, 2012.
- [90] M. Matsuoka, *Infrared Absorbing Dyes*, Springer, New York, NY, USA, 2013.
- [91] J. Lee, M.H. Kang, K.B. Lee, Y. Lee, Characterization of natural dyes and traditional Korean silk fabric by surface analytical techniques, *Materials* 6 (2013) 2007. <https://doi.org/10.3390/ma6052007>.
- [92] C.F. Bohren, D.R. Huffman, *Absorption and Scattering of Light by Small Particles*, Wiley, Louisville, KY, USA, 2008.
- [93] Q. Zhao, J. Zhou, F. Zhang, D. Lippens, Mie resonance-based dielectric metamaterials, *Mater. Today* 12 (2009) 60–69, [https://doi.org/10.1016/S1369-7021\(09\)70318-9](https://doi.org/10.1016/S1369-7021(09)70318-9).
- [94] A.B. Evlyukhin, C. Reinhardt, A. Seidel, B.S. Luk'yanchuk, B.N. Chichkov, Optical response features of Si-nanoparticle arrays, *Phys. Rev. B* 82 (2010), 045404, <https://doi.org/10.1103/PhysRevB.82.045404>.
- [95] L. Cai, Y. Peng, J. Xu, C. Zhou, C. Zhou, P. Wu, D. Lin, S. Fan, Y. Cui, Temperature regulation in colored infrared-transparent polyethylene textiles, *Joule* 3 (2019) 1478–1486, <https://doi.org/10.1016/j.joule.2019.03.015>.
- [96] R. Hu, S. Iwamoto, L. Feng, S. Ju, S. Hu, M. Ohnishi, N. Nagai, K. Hirakawa, J. Shiomi, Machine-learning-optimized aperiodic superlattice minimizes coherent phonon heat conduction, *Phys. Rev. X* 10 (2020), 021050, <https://doi.org/10.1103/PhysRevX.10.021050>.
- [97] X. Wan, W. Feng, Y. Wang, H. Wang, X. Zhang, C. Deng, N. Yang, Materials discovery and properties prediction in thermal transport via materials informatics: a mini review, *Nano Lett.* 19 (2019) 3387–3395, <https://doi.org/10.1021/acs.nanolett.8b05196>.
- [98] Y. Zhang, X. Xu, Machine learning optical band gaps of doped-ZnO films, *Optik* 217 (2020), 164808. <https://doi.org/10.1016/j.ijleo.2020.164808>.
- [99] L. Piloizzi, F.A. Farrelly, G. Marcucci, C. Conti, Machine learning inverse problem for topological photonics, *Commun. Phys.* 1 (2018) 57, <https://doi.org/10.1038/s42005-018-0058-8>.
- [100] X. Liu, C.E. Athanasiou, N.P. Padture, B.W. Sheldon, H. Gao, A machine learning approach to fracture mechanics problems, *Acta Mater.* 190 (2020) 105–112, <https://doi.org/10.1016/j.actamat.2020.03.016>.
- [101] J.D. Evans, F.-X. Coudert, Predicting the mechanical properties of zeolite frameworks by machine learning, *Chem. Mater.* 29 (2017) 7833–7839, <https://doi.org/10.1021/acs.chemmater.7b02532>.
- [102] T.M. Dieb, S. Ju, K. Yoshizoe, Z. Hou, J. Shiomi, K. Tsuda, MDTs: automatic complex materials design using Monte Carlo tree search, *Sci. Technol. Adv. Mater.* 18 (2017) 498–503. <https://doi.org/10.1080/14686996.2017.1344083>.
- [103] G.B. Smith, A. Gentle, P.D. Swift, A. Earp, N. Mronga, Coloured paints based on iron oxide and silicon oxide coated flakes of aluminium as the pigment, for energy efficient paint: optical and thermal experiments, *Sol. Energy Mater. Sol. Cells* 79 (2003) 179–197. [https://doi.org/10.1016/S0927-0248\(02\)00410-5](https://doi.org/10.1016/S0927-0248(02)00410-5).
- [104] G.B. Smith, A. Gentle, P. Swift, A. Earp, N. Mronga, Coloured paints based on coated flakes of metal as the pigment, for enhanced solar reflectance and cooler interiors: description and theory, *Sol. Energy Mater. Sol. Cells* 79 (2003) 163–177, [https://doi.org/10.1016/S0927-0248\(02\)00409-9](https://doi.org/10.1016/S0927-0248(02)00409-9).
- [105] R. Levinson, P. Berdahl, H. Akbari, Solar spectral optical properties of pigments-Part I: model for deriving scattering and absorption coefficients from transmittance and reflectance measurements, *Sol. Energy Mater. Sol. Cells* 89 (2005) 319–349, <https://doi.org/10.1016/j.solmat.2004.11.012>.
- [106] R. Levinson, P. Berdahl, H. Akbari, Solar spectral optical properties of pigments-Part II: survey of common colorants, *Sol. Energy Mater. Sol. Cells* 89 (2005) 351–389, <https://doi.org/10.1016/j.solmat.2004.11.013>.
- [107] S. Wang, T. Jiang, Y. Meng, R. Yang, G. Tan, Y. Long, Scalable thermochromic smart windows with passive radiative cooling regulation, *Science* 374 (2021) 1501–1504. <https://doi.org/10.1126/science.abg0291>.
- [108] K.W. Lee, W. Lim, M.S. Jeon, H. Jang, J. Hwang, C.H. Lee, D.R. Kim, Visibly clear radiative cooling metamaterials for enhanced thermal management in solar cells and windows, *Adv. Funct. Mater.* 32 (2022), 2105882. <https://doi.org/10.1002/adfm.202105882>.
- [109] Z. Zhou, X. Wang, Y. Ma, B. Hu, J. Zhou, Transparent polymer coatings for energy-efficient daytime window cooling, *Cell Rep. Phys. Sci.* 1 (2020), 100231. <https://doi.org/10.1016/j.xcrp.2020.100231>.
- [110] S. Dang, Y. Yi, H. Ye, A visible transparent solar infrared reflecting film with a low long-wave emittance, *Sol. Energy* 195 (2020) 483–490, <https://doi.org/10.1016/j.solener.2019.11.080>.
- [111] A.M. Al-Shukri, Thin film coated energy-efficient glass windows for warm climates, *Desalination* 209 (2007) 290–297, <https://doi.org/10.1016/j.desal.2007.04.042>.
- [112] G.K. Dalapati, S. Masudy-Panah, S.T. Chua, M. Sharma, T.I. Wong, H.R. Tan, D. Chi, Color tunable low cost transparent heat reflector using copper and titanium oxide for energy saving application, *Sci. Rep.* 6 (2016), 20182. <https://doi.org/10.1038/srep20182>.
- [113] A.R. Gentle, G.B. Smith, A subambient open roof surface under the mid-summer sun, *Adv. Sci.* 2 (2015), 1500119, <https://doi.org/10.1002/advs.201500119>.
- [114] W. Li, Y. Shi, K. Chen, L. Zhu, S. Fan, A comprehensive photonic approach for solar cell cooling, *ACS Photonics* 4 (2017) 774–782, <https://doi.org/10.1021/acsp.7b00089>.
- [115] Y. Jin, Y. Jeong, K. Yu, Infrared-reflective transparent hyperbolic metamaterials for use in radiative cooling windows, *Adv. Funct. Mater.* 33 (2023), 2207940, <https://doi.org/10.1002/adfm.202207940>.
- [116] D. Zhao, A. Aili, Y. Zhai, S. Xu, G. Tan, X. Yin, R. Yang, Radiative sky cooling: fundamental principles, materials, and applications, *Appl. Phys. Rev.* 6 (2019), 021306, <https://doi.org/10.1063/1.5087281>.
- [117] J. Mandal, Y. Yang, N. Yu, A.P. Raman, Paints as a scalable and effective radiative cooling technology for buildings, *Joule* 4 (2020) 1350–1356, <https://doi.org/10.1016/j.joule.2020.04.010>.
- [118] X. Li, J. Peoples, Z. Huang, Z. Zhao, J. Qiu, X. Ruan, Full daytime sub-ambient radiative cooling in commercial-like paints with high figure of merit, *Cell Rep. Phys. Sci.* 1 (2020), 100221, <https://doi.org/10.1016/j.xcrp.2020.100221>.
- [119] Y. Chen, B. Dang, J. Fu, C. Wang, C. Li, Q. Sun, H. Li, Cellulose-based hybrid structural material for radiative cooling, *Nano Lett.* 21 (2021) 397–404, <https://doi.org/10.1021/acs.nanolett.0c03738>.
- [120] M. Dong, N. Chen, X. Zhao, S. Fan, Z. Chen, Nighttime radiative cooling in hot and humid climates, *Opt. Express* 27 (2019) 31587–31598, <https://doi.org/10.1364/OE.27.031587>.
- [121] H. Liu, H. Kang, X. Jia, X. Qiao, W. Qjin, X. Wu, Commercial-like self-cleaning colored ZrO₂-based bilayer coating for remarkable daytime sub-ambient radiative cooling, *Adv. Mater. Technol.* 7 (2022), 2101583. <https://doi.org/10.1002/admt.202101583>.
- [122] X. Yang, S. Zhou, X. Zhang, L. Xiang, B. Xie, X. Luo, Enhancing oxygen/moisture resistance of quantum dots by short-chain, densely cross-linked silica glass network, *Nanotechnology* 33 (2022), 465202. <https://doi.org/10.1088/1361-6528/ac86de>.